

Seasonality in Southern Ocean isoscapes

Katie St. John Glew¹, Boris Espinasse², Brian P. V. Hunt³, Evgeny A Pakhomov³, Sarah J Bury⁴, Matt H Pinkerton⁵, Scott D Nodder⁶, Andres Gutierrez-Rodriguez⁶, Karl Safi⁷, Julie C.S. Brown⁷, Laura Graham⁸, Robert B Dunbar⁹, David A. Mucciarone⁹, Sarah Magozzi¹⁰, Christopher J. Somes¹¹, and clive trueman¹

¹University of Southampton

²UiT

³University of British Columbia

⁴NIWA

⁵National Institute of Water and Atmosphere Research

⁶National Institute of Water and Atmospheric Research

⁷National Institute of Water and Atmosphere

⁸University of Birmingham

⁹Stanford University

¹⁰Stazione Zoologica Anton Dohrn

¹¹GEOMAR Helmholtz Centre for Ocean Research

November 21, 2022

Abstract

Polar marine ecosystems are particularly vulnerable to the effects of climate change. Warming temperatures, freshening seawater and disruption to sea ice formation potentially all have detrimental cascading effects on food webs. New approaches are needed to better understand spatio-temporal interactions among biogeochemical processes at the base of Southern Ocean food webs, and how these interactions vary seasonally. In marine systems, isoscapes (models of the spatial variation in the stable isotopic composition) of carbon and nitrogen identify the spatial expression of varying biogeochemical processes on nutrient utilization by phytoplankton. Isoscapes also provide a baseline for interpreting stable isotope compositions of higher trophic level animals in movement, migration and diet research. Here we produce carbon and nitrogen isoscapes across the entire Southern Ocean (>40°S) using surface particulate organic matter (POM) isotope data, collected from multiple sources over the past 50 years and throughout the annual cycle. We use Integrated Nested Laplace Approximation (INLA)-based approaches to predict mean annual isoscapes and four seasonal isoscapes using a suite of environmental data as predictor variables. Clear spatial gradients in $\delta^{13}\text{C}$ and $\delta^{15}\text{N}$ values were predicted across the Southern Ocean, consistent with previous statistical and mechanistic isoscape views of isotopic variability in this region. We identify strong seasonal variability in both carbon and nitrogen isoscapes, with key implications for the use of static or annual average isoscape baselines in animal studies attempting to document seasonal migratory or foraging behaviours.

Seasonality in Southern Ocean isoscapes

Katie St John Glew^{1*}, Boris Espinasse^{2*}, Brian P.V. Hunt^{3,4,5}, Evgeny A. Pakhomov^{4,3,5}, Sarah J. Bury⁶, Matt Pinkerton⁶, Scott D. Nodder⁶, Andres Gutiérrez Rodríguez⁶, Karl Safi⁷, Julie C.S. Brown⁶, Laura Graham^{8,9}, Robert B. Dunbar¹⁰, David A. Mucciarone¹⁰, Sarah Magozzi¹¹, Chris Somes¹², Clive N. Trueman^{1,13}

**K. St John Glew & B. Espinasse are joint first author*

+ B. Espinasse should be contacted as corresponding author (boris.espinasse@laposte.net)

Author's institutional affiliations:

1. School of Ocean and Earth Sciences, University of Southampton, National Oceanography Centre Southampton, European Way, Southampton, SO14 3UH
2. Department of Arctic and Marine Biology, UiT The Arctic University of Norway, Tromsø, Norway.
3. Institute for the Oceans and Fisheries, University of British Columbia, Vancouver BC, V6T 1Z4, Canada
4. Department of Earth, Ocean and Atmospheric Sciences, University of British Columbia, Vancouver BC, V6T 1Z4, Canada
5. Hakai Institute, Tula Foundation, Heriot Bay BC, V0P 1H0, Canada
6. National Institute of Water & Atmospheric Research Ltd (NIWA), Greta Point, 301 Evans Bay Parade, Hataitai, Wellington, New-Zealand, 6021
7. National Institute of Water & Atmospheric Research Ltd (NIWA), Gate 10 Silverdale Road, Hillcrest, Hamilton 3216
8. Geography, Earth and Environmental Sciences, University of Birmingham, UK
9. Biodiversity, Ecology and Conservation Group, International Institute for Applied Systems Analysis, Austria
10. Earth System Science, Stanford University, Stanford, CA 94305.
11. Department of Integrative Marine Ecology, Stazione Zoologica Anton Dohrn, Fano Marine Centre, viale Adriatico 1-N, 61032 Fano, Italy
12. Marine Biogeochemical Modelling, GEOMAR Helmholtz Centre for Ocean Research Kiel, Düsternbrooker Weg 20, 24105 Kiel, Germany
13. Hong Kong Branch of Southern Marine Science and Engineering Guangdong Laboratory (Guangzhou), Hong Kong, China

Key Points

- First carbon and nitrogen isoscape predictions of the entire Southern Ocean, based on particulate organic matter isotope data
- Clear spatial gradients in $\delta^{13}\text{C}$ and $\delta^{15}\text{N}$ values were predicted, consistent with previously reported isotopic variability in this region
- Key implications for the use of isoscape baselines in animal studies attempting to document seasonal migratory or foraging behaviours

Abstract

Polar marine ecosystems are particularly vulnerable to the effects of climate change. Warming temperatures, freshening seawater and disruption to sea ice formation potentially all have detrimental cascading effects on food webs. New approaches are needed to better understand spatio-temporal interactions among biogeochemical processes at the base of Southern Ocean food webs, and how these interactions vary seasonally. In marine systems, isoscapes (models of the spatial variation in the stable isotopic composition) of carbon and nitrogen identify the spatial expression of varying biogeochemical processes on nutrient utilization by phytoplankton. Isoscapes also provide a baseline for interpreting stable isotope compositions of higher trophic level animals in movement, migration and diet research. Here we produce carbon and nitrogen isoscapes across the entire Southern Ocean ($>40^{\circ}\text{S}$) using surface particulate organic matter (POM) isotope data, collected from multiple sources over the past 50 years and throughout the annual cycle. We use Integrated Nested Laplace Approximation (INLA)-based approaches to predict mean annual isoscapes and four seasonal isoscapes using a suite of environmental data as predictor variables. Clear spatial gradients in $\delta^{13}\text{C}$ and $\delta^{15}\text{N}$ values were predicted across the Southern Ocean, consistent with previous statistical and mechanistic isoscape views of isotopic variability in this region. We identify strong seasonal variability in both carbon and nitrogen isoscapes, with key implications for the use of static or annual average isoscape baselines in animal studies attempting to document seasonal migratory or foraging behaviours.

Keywords

Stable isotopes, $\delta^{13}\text{C}$ and $\delta^{15}\text{N}$, POM, Bayesian spatial modelling, migration pathways, trophic baseline

INTRODUCTION

Polar marine ecosystems are impacted disproportionately by ongoing climate change, with repeated observations showing significant ocean warming and freshening trends over several recent decades (Durack & Wijffels, 2010; Sian F. Henley et al., 2020; Schofield et al., 2010; Swart, Gille, Fyfe, & Gillett, 2018). Warming ocean temperatures directly affect sea-ice production and melting rates which play a crucial role in the life cycles of many polar marine animals (Loeb et al., 1997). Further, warming and freshening both affect water column structure (stratification, mixing) and critical biogeochemical processes supporting primary productivity of these regions (Deppeler & Davidson, 2017; Li, McLaughlin, Lovejoy, & Carmack, 2009). Such disruptions at the base of the trophic food web can potentially have large-scale consequences throughout the ecosystem (Sian F. Henley et al., 2020). The Southern Ocean (>40°S) surrounds the Antarctic continent and contains around 15% of the world's ocean surface area, with variable sea-ice cover that results in large marginal ice zones (MIZ). The dominant feature of the Southern Ocean is the eastward flowing Antarctic Circumpolar Current, characterized by a latitudinal gradient in temperature with sharp changes across fronts, separating regions with relatively homogenous physical and chemical properties (Sian F Henley et al., 2020; Orsi & Harris, 2019). The Southern Ocean is a High Nutrient Low Chlorophyll (HNLC) biogeochemical province, with regions of high productivity at frontal zones, on a shallow continental shelf areas around islands and continental landmasses, including Antarctica itself, and in the vicinity of zones of seasonal sea-ice coverage and polynya formation. Primary production in the Southern Ocean supports iconic megafauna and has enabled historic whale and seal fisheries and current fisheries, targeting krill and toothfish, to operate over the past century or more. Changes to the ecosystem structure in the Southern Ocean have the potential to cascade rapidly to higher trophic levels, altering the relative abundance and distribution of top predators (Klein, Hill,

Hinke, Phillips, & Watters, 2018; Reiss et al., 2017; Rogers et al., 2020; Trebilco, Melbourne-Thomas, & Constable, 2020). In this context, the changes in population size of krill, a key species at the base of the food web, is of major concern and led to the creation of the Convention for the Conservation of Antarctic Marine Living Resources (CCAMLR). The combination of climate change and extractive fishery operations has resulted in Southern Ocean ecosystems that are changing rapidly such that observing and predicting anthropogenic ecosystem effects is a pressing priority.

The remote nature of the Southern Ocean makes direct observation of the marine environment and its organisms extremely challenging. Consequently, new approaches are needed to better understand spatio-temporal interactions between biogeochemical processes at the base of Southern Ocean food webs, and the distributions, movements, and diets of mobile consumers. Carbon and nitrogen isoscapes (models of the spatial variation in the isotopic composition of reference materials or animals) have been used in marine ecology to infer spatial distributions in nutrient sources that fuel primary production (Boris Espinasse, Hunt, Batten, & Pakhomov, 2020; MacKenzie, Longmore, Preece, Lucas, & Trueman, 2014), to provide isotopic baselines in trophic studies (Jennings & Warr, 2003; Pethybridge et al., 2018), and to infer animal foraging and migratory movements (Bury et al., In Prep; Ceia et al., 2015; Cherel & Hobson, 2007; Graham, Koch, Newsome, McMahon, & Auriolles, 2010; St John Glew et al., 2018; C. N. Trueman, MacKenzie, & Palmer, 2012). In this context, the development of isoscapes is relevant to a number of topics raised in a community evaluation of priority areas for research in Southern Ocean ecosystems (i.e., see the question cluster: “Antarctic life on the precipice” (Kennicutt et al., 2014)).

Spatial variations in stable carbon isotope ratios ($\delta^{13}\text{C}$) of photosynthesizing phytoplankton are mainly driven by the isotopic composition of the inorganic dissolved carbon source, and the extent of isotopic fractionation during photosynthesis, which varies among phytoplankton species and communities (Goericke & Fry, 1994; Laws, Bidigare, & Popp, 1997; Lee, Schell, McDonald, & Richardson, 2005; Riebesell, Burkhardt, Dauelsberg, & Kroon, 2000). Many of the main factors influencing $\delta^{13}\text{C}$ values of photosynthesizing phytoplankton are influenced indirectly by seawater temperature (Deuser, 1970; Hofmann et al., 2000), leading to close correspondence between spatial variations of $\delta^{13}\text{C}$ values of phytoplankton and sea surface temperature, especially across broad latitudinal gradients (Clive N Trueman & St John Glew, 2019). Stable nitrogen isotope values ($\delta^{15}\text{N}$) vary closely with the availability of nitrogen, primarily in the form of nitrate, and generally increase when nitrogen becomes limiting, providing information on the ecosystem primary productivity and nitrogen sources (DiFiore et al., 2010; G. H. Rau, Low, Pennington, Buck, & Chavez, 1998; Rolff, 2000). The $\delta^{15}\text{N}$ values of primary producers are also strongly influenced by the type of nitrogen available to the system, with recycled nitrogen (ammonium) and fixed N_2 gas (via diazotrophs) generating lower $\delta^{15}\text{N}$ values than new nitrate (Montoya, Carpenter, & Capone, 2002; Ryabenko, 2013; Somes et al., 2010). The relatively high and sequential enrichment of ^{15}N between trophic levels also makes nitrogen isotopes useful tools in defining trophic structure in marine ecosystems (Deniro & Epstein, 1981; Hussey et al., 2014; Post, 2002).

In recent years, global scale mechanistic models have been developed for both $\delta^{13}\text{C}$ and $\delta^{15}\text{N}$, providing valuable information at broad scales to address such issues as seasonality effects and connectivity between large oceanic regions (Magozzi, Yool, Zanden, Wunder, & Trueman, 2017; Somes et al., 2010). In addition, the combination of statistical modeling developments and the increase in available observational data has enabled the production of

165 observation-based isoscapes at relatively fine spatial resolutions, which have been used to
166 resolve local scale physical and biological processes (Boris Espinasse et al., 2020; MacKenzie
167 et al., 2014).

168
169 *In situ* sample-based isoscapes have been produced for some parts of the Southern Ocean
170 (Brault et al., 2018; Jaeger, Lecomte, Weimerskirch, Richard, & Cherel, 2010; Quillfeldt,
171 Masello, McGill, Adams, & Furness, 2010), mainly predicted for one season corresponding to
172 the sampling period, and developed by interpolating values between sample locations. The
173 accuracy of interpolation-based isoscapes is dependent on the resolution and quality of the
174 data coverage, i.e., well covered areas result in meaningful interpolated data, while data from
175 poorly resolved areas should be interpreted with caution (Brault et al., 2018). To improve
176 isoscape accuracy, where sample collection is limited, *in situ* stable isotope data can be
177 combined with measured environmental variables. By statistically modelling the relationships
178 between measured stable isotope values and environmental data, isotope values can be
179 predicted in regions where no isotope samples have been collected (G. J. Bowen, 2010;
180 Gabriel J Bowen & Revenaugh, 2003; Boris Espinasse et al., 2020; St. John Glew, Graham,
181 McGill, & Trueman, 2019).

182
183 In the ocean, stable isotope values of particulate organic matter (POM) have frequently been
184 used as a measure of processes occurring at the base of the food web (Kurle & McWhorter,
185 2017; Somes et al., 2010). Stable isotope values of POM have been widely collected across
186 the Southern Ocean in the last decades for paleontology, physical, biogeochemical and
187 ecological research projects, producing a large number of point observations. Recent studies
188 have highlighted the potential in applying POM stable isotope values in the Southern Ocean
189 to produce isoscapes (Bury, Pinkerton, Williams, St John Glew, & Trueman, in review; B.

190 Espinasse, Pakhomov, Hunt, & Bury, 2019). Such isoscapes could be used in animal
 191 movement studies and more generally to provide insights into the seasonality and spatial
 192 variability of key ecosystem processes such as primary productivity, shifts in phytoplankton
 193 community composition, food web trophic interactions, nitrogen cycling, or sea ice melting
 194 on key ecosystem processes. In this study, we compiled POM $\delta^{13}\text{C}$ and $\delta^{15}\text{N}$ data for the
 195 Southern Ocean from unpublished and published sources and used these data to: 1) build the
 196 first observation-based carbon and nitrogen isoscapes that cover the whole Southern Ocean
 197 ($>40^\circ\text{S}$), and 2) relate seasonality in $\delta^{13}\text{C}$ and $\delta^{15}\text{N}$ spatial distribution to ecological processes.
 198

199 **METHODS**

200 **Data Collection**

201 A meta-analysis was carried out of all published surface POM $\delta^{13}\text{C}$ and $\delta^{15}\text{N}$ data for the
 202 Southern Ocean (defined here to be south of 40°S). Isotope measurements were extracted to
 203 our database if they were georeferenced and with a known sampling date. A list of data
 204 sources including location, date and area of sampling can be seen in Table 1.

205
 206 *Table 1. List of all published datasets containing surface particulate organic matter (POM)*
 207 *carbon ($\delta^{13}\text{C}$) and nitrogen ($\delta^{15}\text{N}$) isotopic data.*

Reference	Year samples collected	Months samples collected	Geographical area	No. of $\delta^{13}\text{C}$ measurements	No. of $\delta^{15}\text{N}$ measurements
Eadie and Jeffrey (1973)	1970	Dec	Indian sector	3	NA
Wada, Terazaki, Kabaya, and Nemoto (1987)	1983-1984	Dec-Jan	South of Australia	2	2
G. Rau, Takahashi, Des Marais, and Sullivan (1991)	1986	Mar	Atlantic sector	28	NA
Altabet and Francois (1994)	1991	Feb	Indian sector	46	46

Francois et al. (1993)	1991	Feb	Indian sector	48	NA
Dehairs et al. (1997)	1991-1992	Oct-Jan	Atlantic/Pacific sectors	44	NA
Bentaleb et al. (1998)	1992	Mar	Indian sector	43	NA
Kennedy and Robertson (1995)	1992	Dec	Pacific sector	51	NA
Riaux-Gobin et al. (2006)	1993	Apr	Indian sector	12	NA
Popp et al. (1999)	1994	Jan	Indian Ocean/South of Australia	56	NA
Trull and Armand (2001)	1994-1996	Jan; Jul; Sep; Nov	South of Australia	198	NA
O'Leary, Trull, Griffiths, Tilbrook, and Revill (2001)	1995	Nov	South of Australia	24	NA
Lourey, Trull, and Sigman (2003) and Lourey, Trull, and Tilbrook (2004)	1997-1998	Dec-Mar; Sep; Nov	South of Australia	169	140
Schmidt et al. (2003)	1999-2000	Mar-Apr	Atlantic sector	4	4
(B. Espinasse et al., 2019)	2004-2006	Apr-May; Nov-Jan; Jun-Jul	Atlantic sector	225	218
Lara, Alder, Franzosi, and Kattner (2010)	2005	Mar-Apr	Argentine shelf-Antarctic peninsula	69	69
Zhang et al. (2014)	2006	Jan	Indian sector	24	NA
Richoux and Froneman (2009)	2007	Apr	Indian sector	2	2
Barrera et al. (2017)	2012	Apr	Drake passage	3	3
Montecinos, Castro, and Neira (2016)	2013	Apr	Pacific sector	2	2
Horii, Takahashi, Shiozaki, Hashihama, and Furuya (2018)	2014	Jan	Pacific sector	1	1
Giménez, Winkler, Hoffmeyer, and Ferreyra (2018)	2014	Feb	Argentine shelf	3	3
Seyboth et al.	2013-2016	Nov-Mar	Antarctic	115	112

(2018)			Peninsula		
--------	--	--	-----------	--	--

208

209 Additional unpublished POM stable isotope data were collected during various cruises
210 conducted in the Southern Ocean over the years 1970 to 2019 and were added to the dataset.
211 All published and unpublished $\delta^{13}\text{C}$ and $\delta^{15}\text{N}$ data are provided in Appendix A. More
212 information about the unpublished data are provided in Appendix B. All water samples for
213 unpublished POM analysis were collected either by pumping surface waters (5-10 m) onboard
214 while underway or using sampling bottles in the upper five meters of the water column. The
215 POM samples were collected by vacuum filtration onto Glass Fibre Filters (GF/F) with a
216 nominal pore size of $\sim 0.7 \mu\text{m}$. Most POM samples were acidified to remove carbonates
217 before being sent for stable isotope analysis. The effect of merging acidified and non-acidified
218 samples is taken into account in the model by including the ‘study’ (i.e., survey) as a random
219 factor. Similarly, carbon isotopic values were not corrected for the Suess effect (Gruber et al.,
220 1999) as the year of sampling is also included in the model structure. A summary of sample
221 distribution per season and per year is provided in Appendix C.

222

223 **Environmental data**

224 We estimated that a 10-year time period was long enough to smooth interannual variability in
225 environmental data (see for example the Southern Annular Mode index) (Marshall 2003). The
226 majority of POM samples were collected during 1995-2015, and a 10-year time period of
227 environmental data was selected between 2005-2015 to predict the most historically recent
228 isoscapes as possible with the data available. Using satellite remote-sensing data a bimonthly
229 climatology was built for this time period, extending across the Southern Ocean from 40°S
230 southwards to the Antarctic continent, and included sea-surface temperature (SST),
231 chlorophyll-*a* (chl*a*) concentration, net primary productivity (NPP), mixed layer depth
232 (MLD), sea-ice concentration, and distance from coast (Dist). Data were provided in various

233 resolutions before being projected onto a one-degree grid. A summary of data sources and
234 value ranges can be found in Appendix D. SST, MLD and sea-ice concentration were
235 retrieved from the Copernicus platform (marine.copernicus.eu/). SST was extracted from the
236 Global ARMOR3D L4 Reprocessed dataset, which provides high resolution temperature and
237 salinity fields derived from *in situ* and satellite observations (Guinehut, Dhomps, Larnicol, &
238 Le Traon, 2012). MLD and sea-ice concentration were issued from the GLORYS12V1
239 product, which is a global ocean eddy-resolving reanalysis covering the satellite altimetry era
240 1993-2018 (more information can be found on the Copernicus platform). Chla concentrations
241 were collected from GlobColour (globcolour.info/). GlobColour delivers a merged product
242 that uses all satellite data available at the processing time (Maritorena, d'Andon, Mangin, &
243 Siegel, 2010). Different models have been developed to produce NPP based on chla
244 concentrations and incident irradiance. It is difficult to reconcile which of these models
245 provides data that are closer to *in situ* observations due to the lack of validation in the
246 Southern Ocean (Strutton, Lovenduski, Mongin, & Matear, 2012). We estimated NPP using
247 the Eppley Vertically Generalized Production Model (Eppley-VGPM) calculation. The
248 Eppley-VGPM calculation is an adaptation of the VGPM approach (Behrenfeld & Falkowski,
249 1997), in which the polynomial description of light-saturated photosynthetic efficiencies as a
250 function of SST is replaced with the exponential relationship described by Morel (1991) and
251 based on the curvature of the temperature-dependent growth function described by Eppley
252 (1972). The code to run the Eppley-VGPM calculation was acquired from Oregon State
253 University (science.oregonstate.edu/ocean.productivity/). The calculation of the net NPP used
254 SST, chla and photosynthetically active radiation (PAR) data (obtained from GlobColour) as
255 inputs. Chla and NPP products are dependent on atmospheric conditions, resulting in missing
256 data for some areas due to persistent cloud coverage. The distance to the coast was calculated
257 as distance from the centre point of the grid cell to the 500 m isobath.

258

259 While the climatology was originally produced at bimonthly resolution, the six austral winter
260 months (May to October) were further merged together as few data were available for this
261 timeframe, and during this period the system is less dynamic due to low light conditions
262 (Arteaga, Boss, Behrenfeld, Westberry, & Sarmiento, 2020). In addition to the seasonal
263 values, a yearly average was calculated. Each environmental covariate value (yearly average
264 and seasonal value) was extracted at each POM sampling location and scaled by subtracting
265 the variable mean from each value and dividing by the variable standard deviation.

266

267 **Isoscape modelling**

268 Isoscapes predicting $\delta^{13}\text{C}$ and $\delta^{15}\text{N}$ values across the Southern Ocean were modelled using a
269 Bayesian hierarchical spatial modelling framework, Integrated Nested Laplace Approximation
270 (INLA), via the R-INLA package (<http://www.r-inla.org>, (Rue, Martino, & Chopin, 2009).
271 This approach was adopted to enable uncertainty due to spatial variability in sample collection
272 seasons and year to be estimated. For a full description of the benefits of the INLA approach
273 in marine isoscape modelling refer to St. John Glew et al. (2019). Values of $\delta^{13}\text{C}$ and $\delta^{15}\text{N}$
274 were modelled as a function of a set of environmental covariates \mathbf{X}_i , with year, season, study
275 and the underlying spatial effect included as random effects. Models were specified as:

276

$$Y_i \sim \text{Intercept} + \boldsymbol{\beta}_i \mathbf{X}_i + f(T_i) + f(U_i) + f(V_i) + f(W_i) + \varepsilon_i$$

277

$$T_i \sim N(0, \sigma_{\text{season}}^2)$$

278

$$U_i \sim N(0, \sigma_{\text{year}}^2)$$

279

$$V_i \sim N(0, \sigma_{\text{study}}^2)$$

280

$$W_i \sim N(0, \Omega)$$

281

$$\varepsilon_i \sim N(0, \sigma^2)$$

282

where Y_i is the isotope value ($\delta^{13}\text{C}$, $\delta^{15}\text{N}$) at location i , \mathbf{X}_i is a vector containing the environmental covariates as linear fixed effects, $\boldsymbol{\beta}$ is a vector of parameters to be estimated, T_i , U_i and V_i are the season, year and study random effects, respectively, with assumed Gaussian distributions, W_i represents the smooth spatial effect, linking each observation with a spatial location, with the elements of the spatial domain Ω estimated using the Matérn correlation, and ε_i contains the independently distributed residuals. All individual POM data were included in the model, including locations where multiple samples were collected at the same location.

Environmental variables to be used in the model (Appendix E) were first selected by performing covariance tests and removing covarying variables with the weakest correlation to both $\delta^{13}\text{C}$ and $\delta^{15}\text{N}$ values. Sea-ice cover and chl a concentration were thus removed from further analysis.

Model selection was based on deviance information criteria and model fit (Pearson's correlation coefficient between predicted and observed values) and was determined by manually running different combinations of covariates and removing the least important covariates in a stepwise process, beginning with the full global model containing all covariates (SST, MLD, PPv, Dist). Twelve-month average environmental variables were used for model selection.

Best-fit models were derived containing both no interaction terms and first order interaction terms (Table 2). Models excluding interaction terms are likely to be more useful for interpreting the most important covariates influencing isotopic variability over larger spatial scales, whereas models containing first order interaction terms are likely to be able to

incorporate smaller scale local variability and predict more precise isoscape models (St. John
Glew, Graham et al., 2019). Non-informative default priors were used for each model.

The best-fit models (both including and excluding interaction terms) were used to predict $\delta^{13}\text{C}$
and $\delta^{15}\text{N}$ values in POM across the whole Southern Ocean spatial domain using continuous
raster surfaces of 12-month averaged, scaled environmental variables as predictors. To ensure
that predicted values fell within a sensible range, environmental variable surfaces were
assessed to check that all values used for predictions fell within the range of values observed
at POM sampling locations. The majority of environmental variable surface values fell within
the observed location range, but any outlier grid cells were clipped from the raster surfaces.
Response variables were estimated at all mesh vertices (Fig. 1), which were then linearly
interpolated within each triangle into a finer regular grid ($2 \times 1^\circ$) via Bayesian kriging. Mesh
maximum edge (triangle size) was selected using a sensitivity analysis, by selecting the
smallest triangle size which notably increased model performance, whilst also accounting for
computing time. Mean and variance predictions were obtained for each grid cell and mapped
to produce carbon and nitrogen isoscapes and model variance surfaces representing expected
average isotopic compositions for POM across the Southern Ocean when accounting for
variability in sample collection year and season. All models were mapped on a polar
projection EPSG 3031 (WDG 84, Antarctic Polar Stereographic).

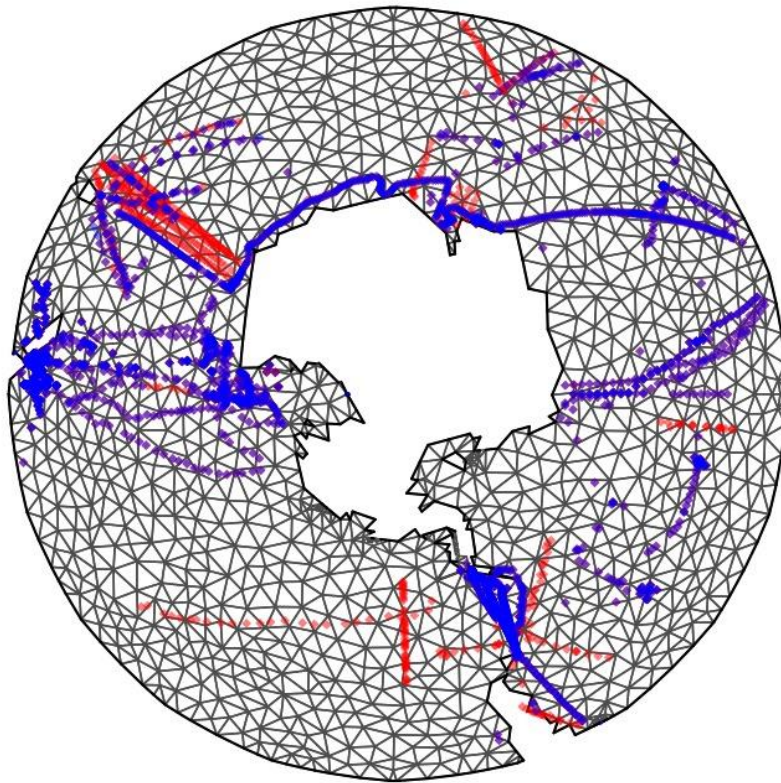


Fig. 1 – Delaunay triangulation mesh for the Southern Ocean: carbon data points = red, nitrogen = blue. Where both carbon and nitrogen data were available points may appear purple.

Seasonal differences

Four different methods were explored to model the seasonal carbon and nitrogen isotopic differences within the Southern Ocean. Firstly, the universal models (using the same covariate terms and coefficient values as the mean models), including season as a random effect, were run on all data including all seasons and subsequently used to predict season-specific isoscapes using season-specific environmental data. Secondly, season was included in the model above as a covariate fixed effect rather than a random effect. Thirdly, models including the universal covariate terms, but excluding season, were run on season-specific data enabling the coefficient terms to vary between seasons. These season-adjusted models were then used

to predict seasonal isoscapes by applying season-specific environmental data. Finally, new best-fit no-interaction and first order interaction models were derived for each season for both carbon and nitrogen, using season-specific environmental data. Details of the best-fit models can be seen in Appendix F.

The first two methods coped with the patchy data distribution between seasons better, with low model variability ($<0.8\%$ for carbon and $<1.5\%$ for nitrogen), however they likely underestimated seasonal isotopic differences across the spatial domain. On the other hand, while season-specific best-fit model predictions were likely to be most accurate and precise, they were more strongly influenced by the spatial differences in seasonal data distribution, with larger model variance values (up to 80%) observed in regions lacking data. Seasonal isoscape surfaces for all methods can be compared in Appendix G. The third method, using universal covariate terms adjusted for each season, was selected as a compromise between predicting accurate and precise seasonal isoscapes, yet realistic in regions with little data coverage. Predicted isoscape surfaces for March-April (autumn), May-October (winter) and November-December (spring) were then subtracted from the January-February (summer) isoscapes (the season with the highest number of data points) for both carbon and nitrogen (no-interaction and interaction model predictions) to demonstrate seasonal variability in $\delta^{13}\text{C}$ and $\delta^{15}\text{N}$ values across space.

RESULTS

POM data

In total, 3237 carbon and 2614 nitrogen POM data points were compiled from across the Southern Ocean at 2766 and 2215 locations, respectively (Fig 2). Data were collected across 31 different years from 1970 – 2019, with most data collected from 1995 - 2015. Data were

collected across all seasons, with most samples collected in January-February during the austral summer (Fig. 2). No strong spatial bias in sample collection season was observed, with many regions sampled across multiple seasons (Fig. 2). The $\delta^{13}\text{C}$ and $\delta^{15}\text{N}$ value ranges of all POM samples were -36.84‰ to -16.49‰ and -6.09‰ to +10.80‰, respectively.

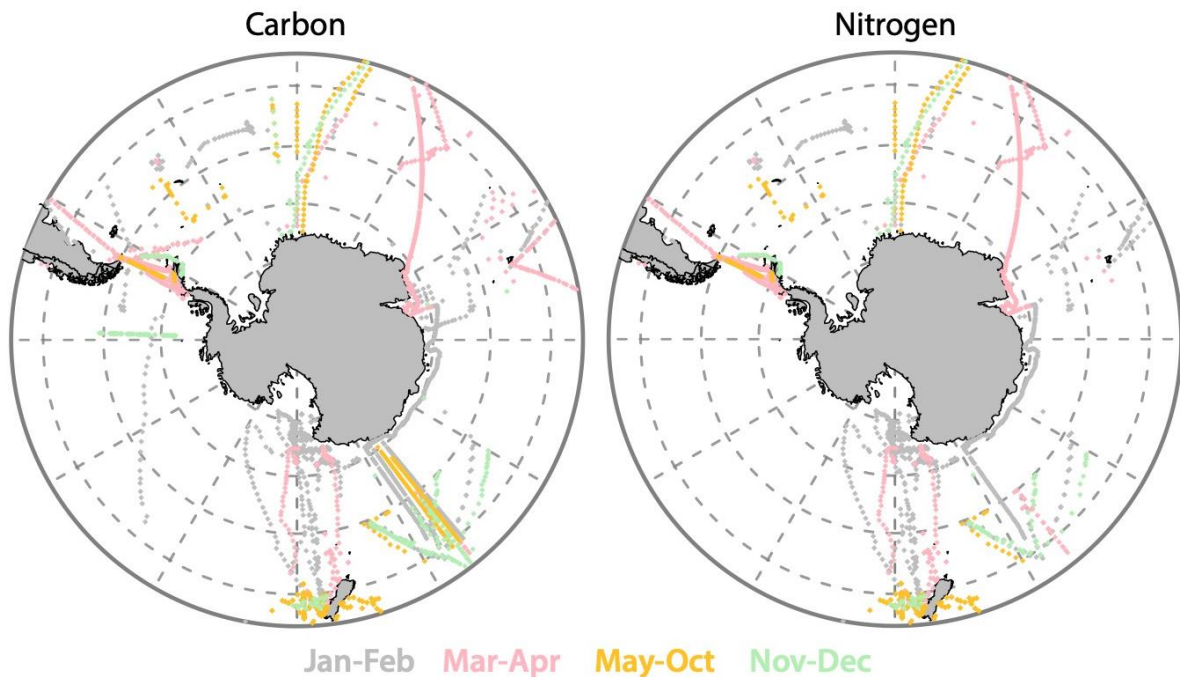


Fig. 2. Locations of surface particulate organic matter (POM) samples for carbon ($\delta^{13}\text{C}$) and nitrogen ($\delta^{15}\text{N}$) isotope analysis, collected across the Southern Ocean in Jan-Feb (grey), Mar-Apr (pink), May-Oct (yellow) and Nov-Dec (green).

Southern Ocean isoscape models

The best-fit carbon and nitrogen prediction models, both excluding and including first order interaction terms, are displayed in Table 2. The strongest covariate predictors for $\delta^{13}\text{C}$ variability were SST, NPP and MLD. The same covariates, with the addition of distance from land, were significant predictors for $\delta^{15}\text{N}$ variability. The best-fit models were able to explain 86% and 74-76% (correlation coefficient) of the spatial variability observed in carbon and nitrogen isotopes, respectively (Table 2).

383

384 *Table 2. Best-fit (no interaction and first order interaction) models for surface particulate*
 385 *organic matter (POM) carbon ($\delta^{13}\text{C}$) and nitrogen ($\delta^{15}\text{N}$) isotope values with environmental*
 386 *covariates (SST = Sea Surface Temperature, Dist = Distance from land, NPP = net primary*
 387 *production, MLD = mixed layer depth) and fixed effects of year and season*
 388 *(January/February, March/April, May-October, November/December), with associated*
 389 *deviance information criteria (DIC) values and correlation coefficients of predicted values*
 390 *against measured values. The precision (Precision = 1/variance) mean and credible interval*
 391 *for each random effect term are also stated.*

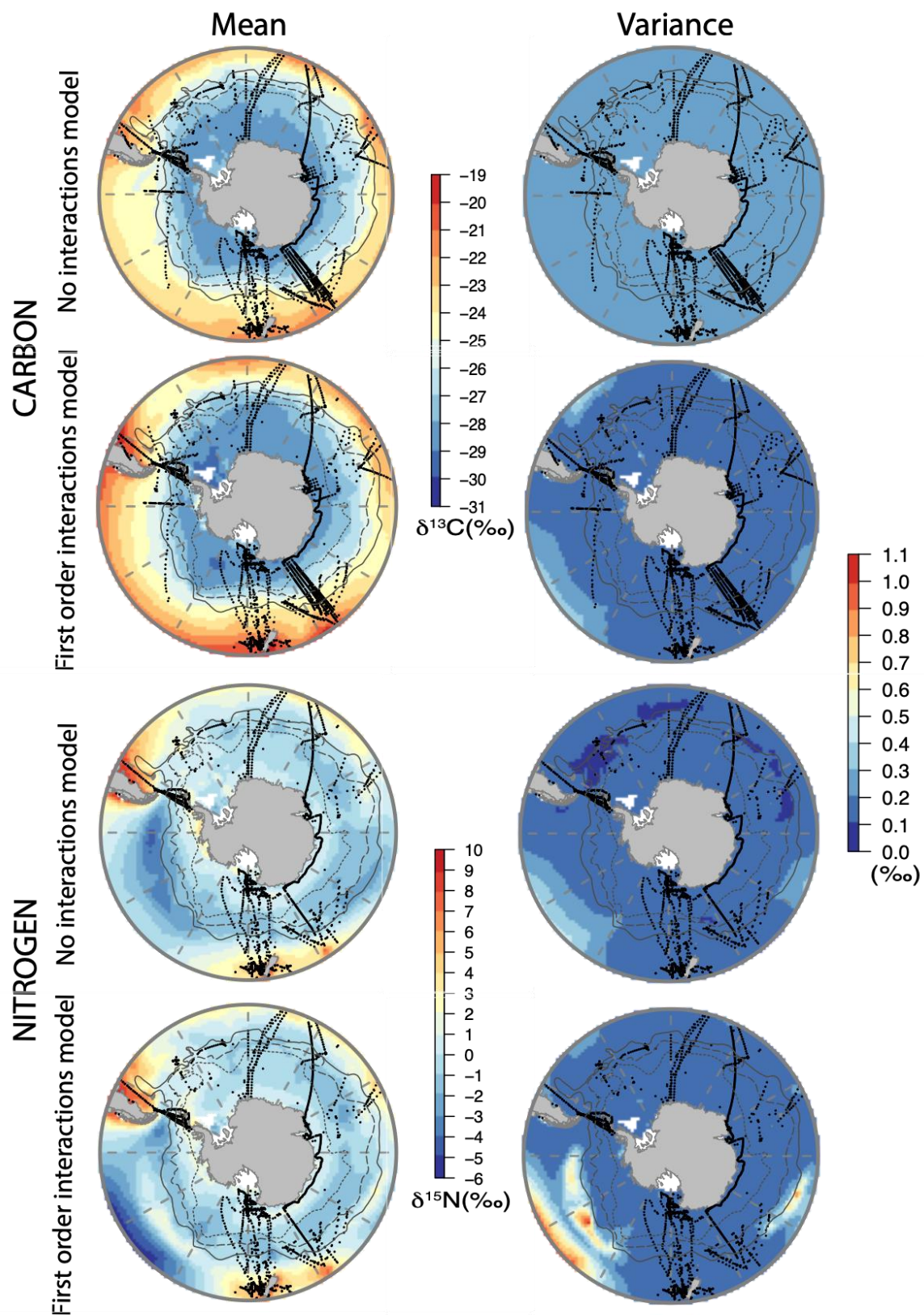
Model	DIC	Correlation Coefficient	Random Effects Precision (Mean (credible intervals))		
			Season	Year	Study ID
$\delta^{13}\text{C} \sim -25.8 + 2.28*\text{SST} + 0.27*\text{NPP} + 0.01*\text{MLD} + \text{f}(\text{Year}) + \text{f}(\text{Season}) + \text{f}(\text{Study})$	12818	0.86	11.5 (2.3,32.5)	0.9 (0.5, 1.4)	0.4 (0.2, 0.7)
$\delta^{13}\text{C} \sim -26.2 + 2.82*\text{SST} - 0.51*\text{NPP} - 0.22*\text{MLD} - 0.68*\text{Dist} - 0.42*\text{SST:NPP} - 0.34*\text{MLD:NPP} - 0.76*\text{Dist:NPP} + \text{f}(\text{Year}) + \text{f}(\text{Season}) + \text{f}(\text{Study})$	12646	0.86	4.5 (1.0, 12.8)	1.5 (0.9, 2.2)	0.5 (0.3, 0.7)
$\delta^{15}\text{N} \sim 0.09 + 0.89*\text{NPP} - 0.88*\text{MLD} - 0.46*\text{Dist} + 0.4*\text{SST} + \text{f}(\text{Year}) + \text{f}(\text{Season}) + \text{f}(\text{Study})$	11235	0.74	16.6 (1.2, 86.1)	2.8 (1.2, 6.0)	0.9 (0.4, 1.8)
$\delta^{15}\text{N} \sim -0.07 + 1.19*\text{NPP} - 0.26*\text{MLD} - 0.49*\text{Dist} + 0.27*\text{SST} + 0.4*\text{SST:NPP} + 0.79*\text{MLD:Dist} + 0.7*\text{MLD:NPP} + \text{f}(\text{Year}) + \text{f}(\text{Season}) + \text{f}(\text{Study})$	11072	0.76	5.9 (5.3, 5.3e ⁵)	2.0 (1.1,3.7)	0.7 (0.2,1.5)

392

393 Spatial distributions of $\delta^{13}\text{C}$ data across the Southern Ocean are largely consistent with
 394 previous research showing relatively low $\delta^{13}\text{C}$ values at higher latitudes (-31‰ to -28‰) and
 395 gradually increasing with distance from the polar region to values of -24‰ to -20‰ at 40°S
 396 (Fig. 3). Higher $\delta^{13}\text{C}$ values are also predicted closer to land (-22‰ to -19‰), both east and
 397 west of southern South America and New Zealand. Spatial distributions of $\delta^{15}\text{N}$ across the
 398 Southern Ocean varied between sectors, with relatively negative $\delta^{15}\text{N}$ values observed in the
 399 Pacific Ocean sector (-6‰ to -1‰), compared to slightly more positive values observed in the

Atlantic (-1‰ to 4‰) and Indian ocean sectors (-2‰ to 1‰). Notably higher $\delta^{15}\text{N}$ values (3‰ to 10‰) were predicted in the vicinity of land masses, both east and west of southern South America, around New Zealand, and south of Tasmania (Fig. 3).

Variance surfaces show broadly similar patterns for both carbon and nitrogen models, with less than 0.4‰ uncertainty values across the majority of the Southern Ocean (Fig. 3). For both carbon and nitrogen isoscapes, predictions based on the models including first order interactions increased the predicted isotopic range and spatial differences at more local resolutions. Introduction of interaction terms also increased uncertainty values from less than 0.4‰ up to approximately 1‰ in certain regions, such as within waters leading to the Pacific Ocean and Indian Ocean, where *in situ* data samples are scarce (Fig. 3).



413

414 *Fig. 3. Southern Ocean surface particulate organic matter (POM) carbon ($\delta^{13}\text{C}$) and nitrogen*

415 *($\delta^{15}\text{N}$) 12-month average isoscape predictions, derived from models both excluding and*

including interaction terms, and the associated variance of the posterior predicted distribution, after seasonal and yearly random effects have been accounted for. Black dots represent sample locations. Paths of the Southern Ocean fronts are shown in dark grey (solid line; Sub-Antarctic Front, dashed line; Polar Front and dotted line; southern Antarctic Circumpolar Current Front as described by Orsi and Harris (2019)).

Seasonal differences

Similar residual isotopic variability between seasons was observed in all $\delta^{13}\text{C}$ and $\delta^{15}\text{N}$ models, with approximately 1‰ difference between seasons not accounted for by the variables in the selected models (Fig. 4). Within the $\delta^{13}\text{C}$ models, isotopic differences occurring during the January and February summer months were most different to the remainder of the year, with positive residual values in comparison to the winter months (May-October). Within the $\delta^{15}\text{N}$ models, isotopic residual values were most different in spring (November-December), with higher unexplained values compared to the rest of the year (Fig. 4).

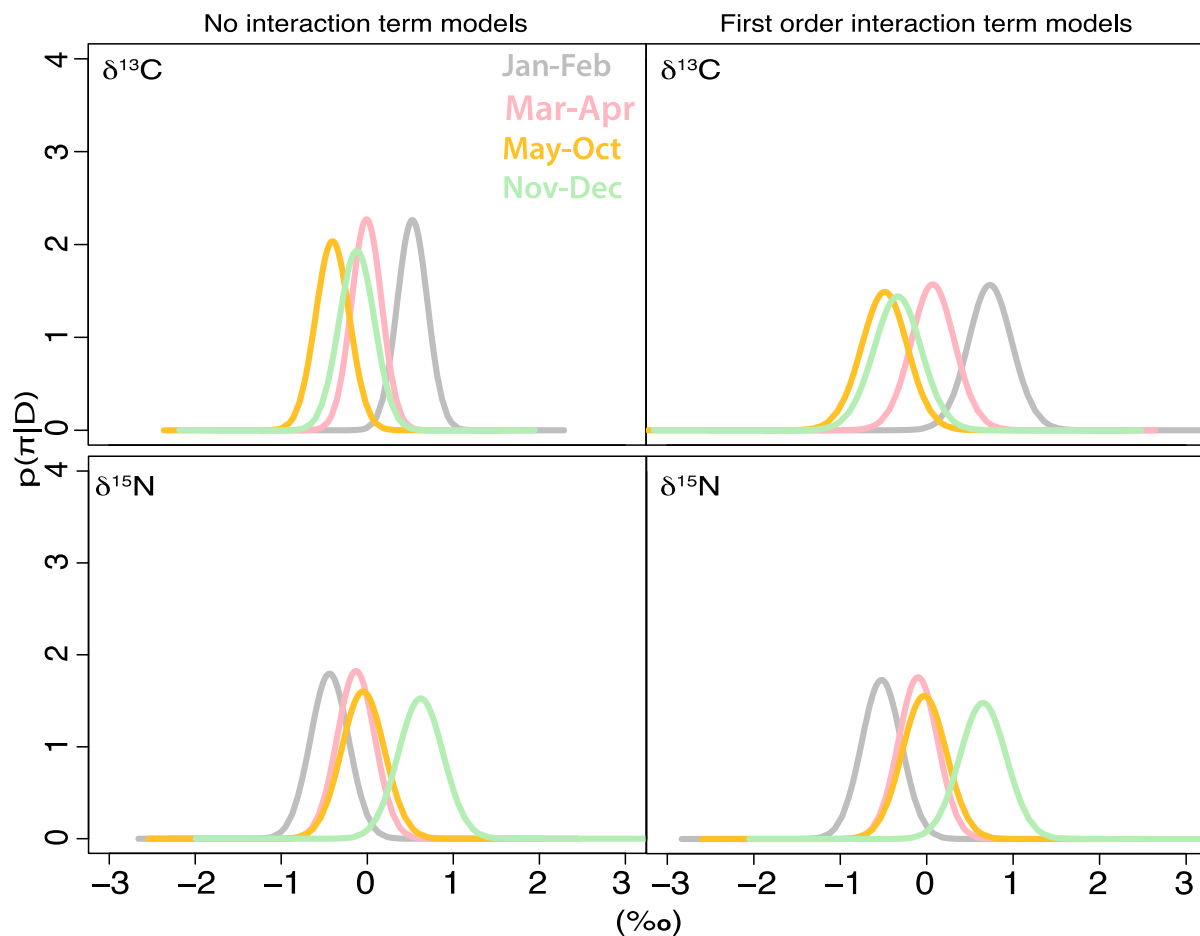


Fig. 4. Marginal posterior distributions of the seasonal random effect for the selected carbon ($\delta^{13}\text{C}$) and nitrogen ($\delta^{15}\text{N}$) isoscape prediction models (both excluding and including first order interaction terms). The symbol π is the seasonal - level deviation from the overall mean isotope value, and D represents data. Distributions represent the probability density of a given isotopic difference, given the data, and represents seasonal differences that remain after the models have been applied.

Carbon isotope values were predicted to vary between season by approximately $\pm 4\text{‰}$ on average, but up to $\pm 8\text{‰}$ in certain regions (Fig. 5). In the most northerly regions of the Southern Ocean, the highest $\delta^{13}\text{C}$ values were predicted in both carbon models during the summer months of January and February. In the more southerly regions, surrounding Antarctica, the highest values were predicted in March and April, with the lowest $\delta^{13}\text{C}$ values

predicted in peak summer months. Overall, the lowest $\delta^{13}\text{C}$ values were predicted in winter months (May-October), particularly within the Pacific Ocean (Fig. 5).

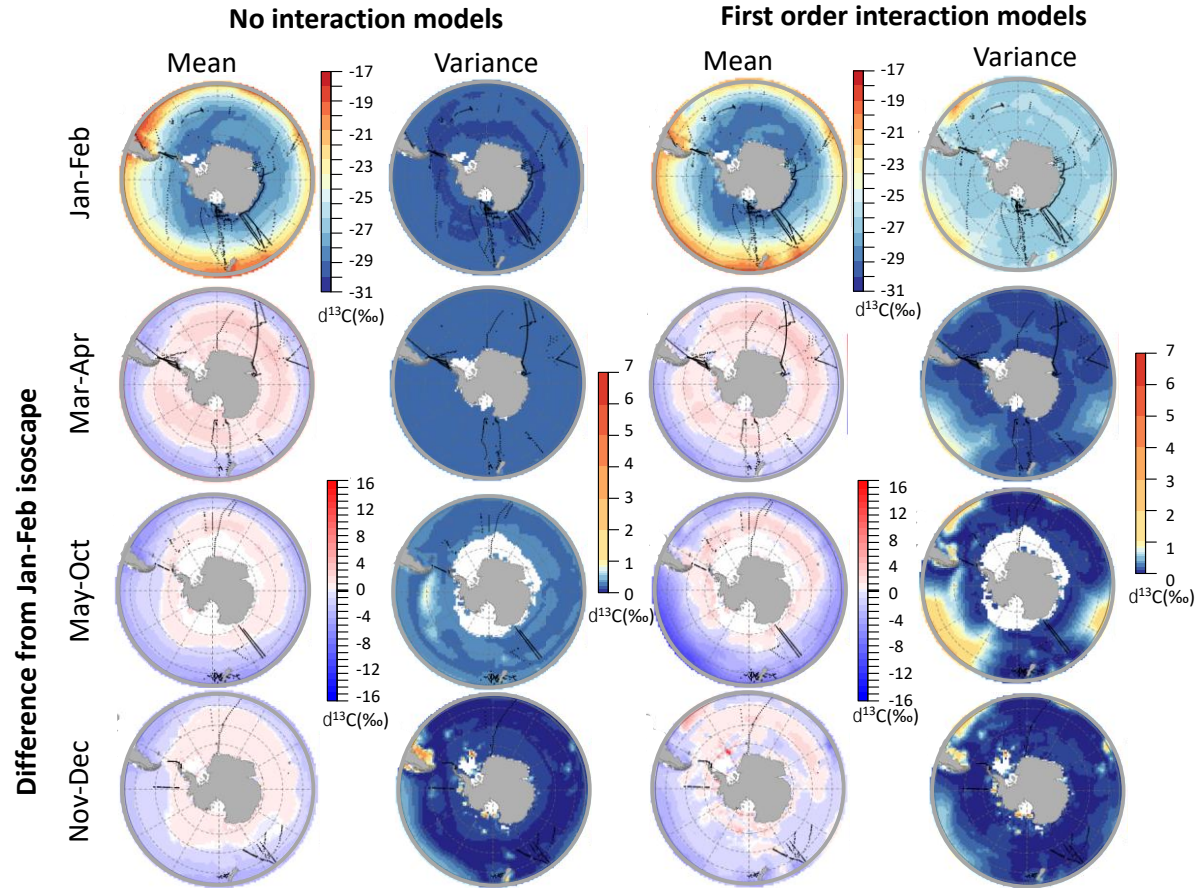


Fig. 5. January – February summer season-specific carbon ($\delta^{13}\text{C}$) non-interaction term and first order interaction term isoscape prediction. The spatial isotopic differences of each season compared to the Jan-Feb prediction (each season prediction minus Jan-Feb prediction) are also shown. Blue areas depict regions which are predicted to have lower carbon isotope values compared to January and February, and red areas depict regions which are predicted to have higher $\delta^{13}\text{C}$ values during that season. Variance surfaces for each seasonal model prediction are also shown. Data points are shown as black dots.

Nitrogen isotope values were predicted to vary between seasons more than carbon isotope values, with average isotopic differences of $\pm 4\%$, but with differences of up to $\pm 16\%$

459 occurring in some regions, such as the open ocean regions of the Pacific and Indian sectors
460 and east of Argentina (Fig. 6). The highest $\delta^{15}\text{N}$ values were predicted in spring (November-
461 December) across the majority of the Southern Ocean. An exception was the area east of
462 Argentina, where the highest $\delta^{15}\text{N}$ values were predicted to occur in summer (January-
463 February). Nitrogen isotope values were predicted to be relatively low during the autumn
464 months (March–April) across the majority of the Southern Ocean. Values of $\delta^{15}\text{N}$ were
465 predicted to be rather variable in winter months, exhibiting values that may be either lower or
466 higher than those predicted for summer months. The two model types also predicted different
467 patterns, with extremely low $\delta^{15}\text{N}$ values (-16‰ to -2‰) predicted in the open ocean areas in
468 the no-interaction models, but extremely high $\delta^{15}\text{N}$ values (8‰ to 16‰) predicted in the first
469 order interaction model (Fig. 6).

471 Isoscape model variance values for carbon in all seasons and for nitrogen in January-February
472 and March-April were relatively low with values in most areas being less than 2‰. There was
473 increased variance for both carbon and nitrogen within the open ocean areas of the Pacific and
474 Indian Oceans where limited data were collected. The highest carbon and nitrogen variance
475 values were observed in the winter (May-October) isoscape predictions where fewer POM
476 samples were collected compared to all other seasons. First order interaction models had
477 greater variance values than the no interaction models.

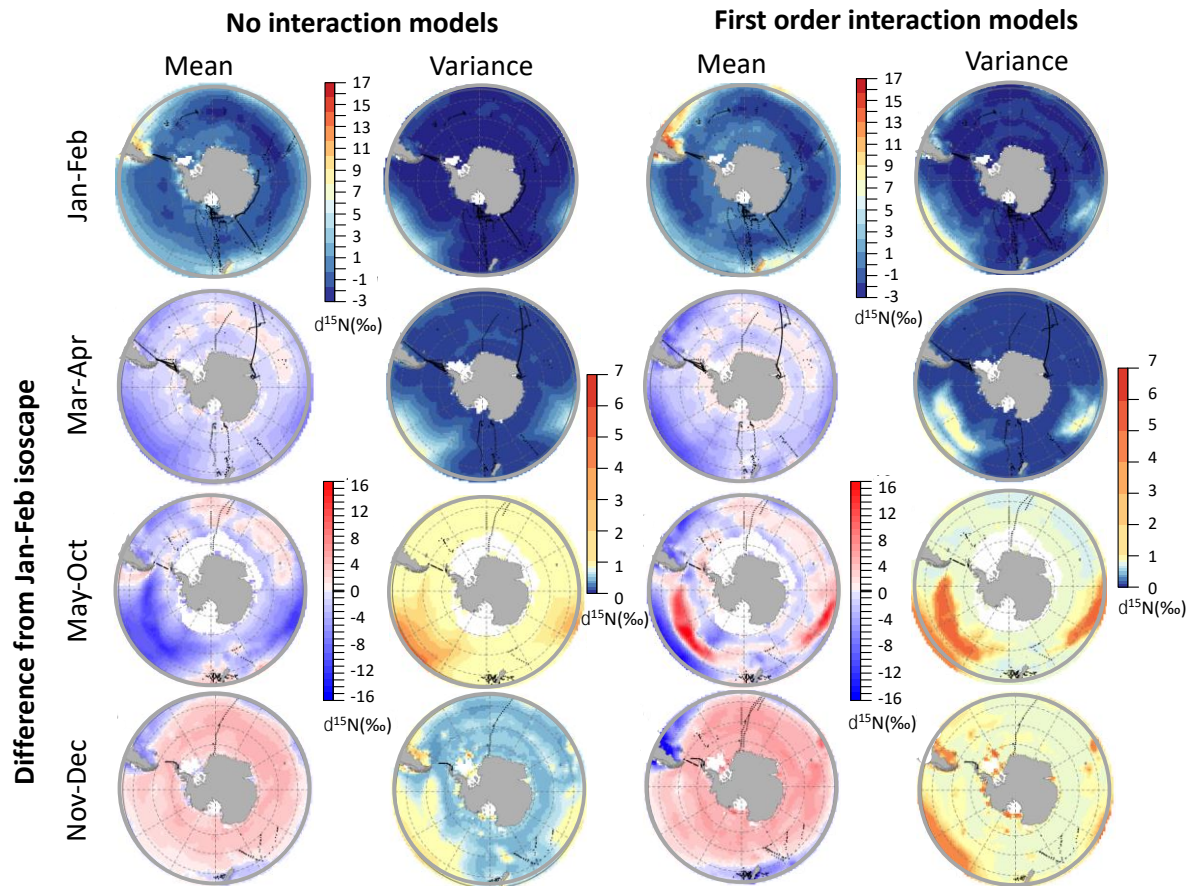


Fig. 6. January – February season-specific nitrogen non-interaction term and first order interaction term isoscape prediction. The spatial isotopic differences of each season compared to the Jan-Feb prediction (each season prediction minus Jan-Feb prediction) are also shown. Blue areas depict regions which are predicted to have lower nitrogen isotope values compared to January and February, and red areas depict regions which are predicted to be higher in $\delta^{15}\text{N}$ during that season. Variance surfaces for each seasonal model prediction are also shown. Data points are shown as black dots.

DISCUSSION

This study provides a significant improvement in the prediction of carbon and nitrogen isoscapes across the Southern Ocean, in comparison to previously produced global mechanistic model predictions (Magozzi, Yool et al. 2017, Somes, Schmittner et al. 2010) and regional scale sample-based predictions (Brault et al., 2018; Jaeger et al., 2010; Quillfeldt et

al., 2010). The yearly modelled $\delta^{13}\text{C}$ values were strongly driven by temperature, decreasing towards the pole, following the expected gradient of increasingly more negative isotopic values towards the polar latitudes (Goericke & Fry, 1994; Quillfeldt et al., 2010; G. Rau et al., 1991). Changes across longitude mainly tracked North/South variations in the position of the Polar Front. Elevated $\delta^{15}\text{N}$ values coincided with areas of higher primary production, generally located down-current (east) of land masses or islands or above continental shelves that extend around the continents and islands of the Southern Ocean.

Seasonal modelled carbon and nitrogen isoscapes had higher variability in predicted values than the 12-month averaged isoscapes, particularly for winter/spring months, which were commonly under sampled. Values of $\delta^{13}\text{C}$ were largely driven by surface ocean temperatures, with higher $\delta^{13}\text{C}$ values predicted earlier in the seasonal cycle at lower latitudes, where temperatures were warmer. Maximum $\delta^{13}\text{C}$ values in January-February were predicted north of the Polar Front, but March-April maximum values occurred to the south. Nitrogen isotope values peaked in November-December (spring), corresponding to high pelagic production at low latitudes, coinciding with the release of nutrient-enriched water from sea-ice melt at high latitudes.

$\delta^{13}\text{C}$ spatial and seasonal variability

As expected, SST, as the driver for CO_2 concentration in seawater, was the predominant factor explaining geographic and seasonal changes in $\delta^{13}\text{C}$ values in our model, with a large range of measured SST values and predicted $\delta^{13}\text{C}$ values from 40°S to the Antarctic continent. The second key predictor of $\delta^{13}\text{C}$ variability was net primary production. While both primary productivity and chl *a* concentrations from satellites were considered as potential predictors early in the modelling process, primary productivity emerged to be a more powerful predictor.

The approach for estimating primary productivity took into account several parameters such as irradiance and temperature, and also includes a temperature-dependent description of photosynthetic efficiencies (Behrenfeld & Falkowski, 1997). The amount of light in the Southern Ocean varies significantly with latitude, and also mixed layer depth, and this will affect photosynthetic efficiency (Bracher, Kroon, & Lucas, 1999). By taking into account latitudinal changes in daily irradiance and temperature, primary productivity might better correlate with seasonal and spatial variations in phytoplankton physiology and primary production rates, which in turn affect carbon uptake and thus $\delta^{13}\text{C}$ values over the wide latitudinal range covered in this study.

The predicted $\delta^{13}\text{C}$ values presented in this study are comparable to the values modelled by Magozzi et al. (2017). Both carbon isoscapes predicted a similar range of values (-20‰ to -30‰) with higher values at low latitudes such as around the continental shelves of South America and Tasmania/New Zealand and lower values found within the Weddell and Ross seas (Fig. 3). Overall, the Magozzi, Yool et al. (2017) model predicted lower $\delta^{13}\text{C}$ values with a median offset of 2‰. Including first order interactions, our INLA model produced a better match between statistical and mechanistic isoscape models, with interaction terms removing extreme $\delta^{13}\text{C}$ values predicted east and west of South America. Including first order interaction terms reduced the standard deviation of the offset between statistical and mechanistic isoscape models from 1.2 to just 0.6‰ (Appendix H). The estimated inter-seasonal variability was also comparable with a range of 6‰ at 60°S modelled by Magozzi et al. (2017) and seasonal anomalies mainly between -4‰ and 4‰ in the present study (Fig. 5). However, we observed a slight temporal offset in peak $\delta^{13}\text{C}$ value timings: at location 60°S/-90°E, with maximum values predicted in January-February by Magozzi et al. (2017) compared to March-April in our study. In general, south of the Polar Front, $\delta^{13}\text{C}$ values were

relatively stable between seasons, most likely due to limited variation in water temperatures within this region. The model did not fully depict the high variability in $\delta^{13}\text{C}$ values sometimes observed in this area (Munro, Dunbar, Mucciarone, Arrigo, & Long, 2010). High variability can be due to the release of brine waters from ice melting, which are enriched in ^{13}C (Munro et al., 2010), and promote phytoplankton development due to increased iron input (Lannuzel et al., 2016). North of the Polar Front, highest $\delta^{13}\text{C}$ values were predicted in summer (January-February), in agreement with the temperature cycle in this region. Very low values were predicted in the Pacific Ocean during winter, although these values were associated with high uncertainties and should therefore be taken with caution. Another noteworthy feature was that the $\delta^{13}\text{C}$ values on the Patagonian shelf were predicted to peak early in the year, potentially as a result of the phytoplankton bloom happening in October (considered in this study as a winter month) (Carreto et al., 2016), earlier than in other areas at a similar latitude. Intense phytoplankton blooms can lead to increased $\delta^{13}\text{C}$ values by locally decreasing the concentration of aqueous CO_2 (Deuser, 1970). It should be noted, however, that these values were also associated with high uncertainties and should be interpreted with caution.

$\delta^{15}\text{N}$ spatial and seasonal variability

Primary productivity and mixed-layer depth were the two main factors driving $\delta^{15}\text{N}$ variability in our model. Both are important processes in controlling the concentration and availability of nitrogen-based nutrients in the euphotic layer. Phytoplankton uptake of nutrients for growth will diminish the nutrient pool, while wind mixing and high energetics of the ACC (Sokolov & Rintoul, 2009) will replenish the nutrient pool by mixing deep, nutrient-rich water into the surface layer. The degree of mixing is positively correlated with mixed-layer depth, although it is not necessarily true at small time scale (Franks, 2015). Nitrate

concentrations in the Southern Ocean are generally higher south of the Polar Front and decrease north of the Polar Front (Switzer, Kamykowski, & Zentara, 2003) where primary productivity is on average greater. The mixed-layer depth was highest in the open ocean zone south of the Polar Front. This allows for euphotic zone nitrate replenishment but the deep mixed layer depth can also result in light limitation of phytoplankton growth (Deppeler & Davidson, 2017). The mixed-layer depth gets shallower south of the southern Antarctic Circumpolar Current Front, especially in the marginal ice zone during sea ice melt.

The two other factors playing a role in $\delta^{15}\text{N}$ variability were distance to land and SST. Coastal environments are usually characterised by higher carbon and nitrogen stable isotope values that decrease with distance offshore (Kline Jr, 2009; Lara et al., 2010; Zhang et al., 2014). The drop in $\delta^{13}\text{C}$ values is usually sharp, occurring in the near coastal area, but $\delta^{15}\text{N}$ values can remain high over tens to a few hundred kilometres from the coast depending on surface water advection (El-Sabaawi, Trudel, Mackas, Dower, & Mazumder, 2012). A potential explanation is that ^{12}C within surface waters are able to be readily replenished by atmospheric exchange, while replenishment of ^{14}N within surface waters is mostly dependent on mixing with deeper waters and, therefore, is dependent on mixing conditions. This may potentially explain why distance to coast is a significant predictor in the nitrogen model, but not in the carbon model. SST likely plays an indirect role in $\delta^{15}\text{N}$ variation, by acting as a proxy for the latitudinal increase of nutrient availability from north to south (Switzer et al., 2003).

The combination of the four principle factors (NPP, MLD, SST and Dist) result in the delineation of two distinctly different biogeochemical regimes, north and south of the Polar Front. North of the Polar Front, $\delta^{15}\text{N}$ values varied closely with the intensity of primary production as the lower starting levels of nitrate are more prone to depletion and

correspondingly, an increase in phytoplankton $\delta^{15}\text{N}$ values. South of the Polar Front, $\delta^{15}\text{N}$ values are low in the open ocean but increase in the marginal ice zone where meltwater can result in shallower mixed layer depths constraining nutrient rich waters in the photic zone. The release of micronutrient such as iron will promotes phytoplankton growth and associated nitrates uptake (Lannuzel et al., 2016; Tagliabue et al., 2017). Sea-ice concentration, although thought to be an important factor, was removed from the model due to a strong correlation with SST. Sea-ice concentration may be a stronger predictor of $\delta^{15}\text{N}$ values if just focusing on the region south of the Polar Front, however, for the whole Southern Ocean, SST was proven to be a more powerful predictor.

It is notoriously difficult to model nitrogen isoscapes based on a mechanistic approach. Somes et al. (2010) were the first to do so at a global scale, predicting $\delta^{15}\text{N}$ values varying between 0‰ and 6‰ south of 40°S, which is a narrower range than predicted here (-2‰ to 8‰) (Appendix H). Offsets between statistical and mechanistic nitrogen isoscapes varied over a large 15‰ range, highlighting the complexity of nitrogen isotope dynamics. In general, statistical interpolation models predicted higher $\delta^{15}\text{N}$ values than mechanistic models at the margins of the Antarctic continent, around the Patagonian shelf and Scotia Arc. This is potentially due to increased predictive precision within highly productive areas where the uptake of nitrate results in high $\delta^{15}\text{N}$ values that may not be captured in the mechanistic model. By contrast, the mechanistic model predicted higher $\delta^{15}\text{N}$ values than statistical observation at higher latitudes. In contrast to the Somes, Schmittner et al. (2010) nitrogen isotope model, INLA models that allow first order interactions produced greater variance between statistical and mechanistic nitrogen isoscapes (standard deviation of offset values: 2.6‰ for no interaction model and 3.25‰ for the interaction model).

The modelled seasonal changes in $\delta^{15}\text{N}$ values should be considered carefully because models suggested high uncertainties for winter (May-October) and spring (November-December) (Fig. 6). Seasonal isoscape predictions showed higher $\delta^{15}\text{N}$ values occurring in November-December for a large part of the Southern Ocean, excluding productive areas over continental shelves. Even though the Southern Ocean is a High Nutrient-Low Chlorophyll region, where phytoplankton development is mainly limited by iron inputs (Boyd et al., 2000; Martin, 1990; Trull & Armand, 2001), the decrease of the nitrate pool during the spring bloom is followed by an increase in $\delta^{15}\text{N}$ values in POM (DiFiore et al., 2010). Furthermore, the melting of the sea-ice is associated with a release of sea biota (phyto- and microzooplankton), which are enriched in ^{15}N (Fripiat et al., 2014). As this process is not directly translated into the model (Table 2), it could be the cause of higher $\delta^{15}\text{N}$ values, which are unexplained by the model for spring (November-December) (Fig.4).

Model structure

In this investigation, two different statistical isoscape models were built and presented; 1) including, or 2) excluding first order interactions terms between environmental predictor variables in the model structure. Including interaction terms enabled a larger range of isotope predictions and associated variance to be captured, but also complicates the model structure and therefore interpretation of the outputs. The simpler, no-interaction term models allowed for manageable interpretation of model relationships between the covariate and dependent variables, which could then be aligned to known ecological processes, as discussed above. Simple, no-interaction term isoscapes are useful for comparing broad-scale differences in isotopic ratios across space and for studies describing the underlying physical and biogeochemical mechanisms responsible for spatio-temporal variations in stable isotope values. Models including interaction terms explain more of the variance observed in data and

therefore produced more precise and potentially more accurate spatial isotopic predictions. Accurate and precise isoscapes are particularly valuable for animal geolocation studies (Cherel & Hobson, 2007; Clive N Trueman & St John Glew, 2019), especially when identifying the organism's origin using relatively fast turnover tissues (blood plasma, muscles) (Jaeger et al., 2010), or piecing together migration history by performing high-resolution sampling of calcified tissues (e.g. otoliths) (Darnaude & Hunter, 2018; Sakamoto et al., 2018; C. N. Trueman et al., 2012). The underlying spatial structure in the isoscape model uncertainty (variance isoscapes) are also critical for animal assignment studies, highlighting the regions where isoscape predictions are less accurate either due to limited data availability, locally high variance in predictor variables, or predictor values in the projected region which are out of the range of those in the observed areas. Spurious prediction can also be the result of a combination of limited data and strong influential interaction. For example, within the Pacific Ocean, winter predictions of high $\delta^{15}\text{N}$ POM values are related to deep mixed-layer depth (>300 m depth) and low primary productivity but are hard to relate to ecological processes. Assuming that uncertainty terms are included in an assignment process, it will always be more difficult to assign an individual or population of individuals to a region where the isoscape prediction has higher uncertainty, even if the isotope values of the isoscape and assignment animal tissue are a close match (Wunder, 2010).

The results presented here highlight the need for baseline seasonal isotopic variability to be accounted for when using isoscapes for animal assignment purposes. In the present study, both carbon and nitrogen values varied significantly within the same geographic location between seasons, with variations of up to approximately 10‰ for nitrogen and 4‰ for carbon. The strength of isotopic differences between geographic regions within the Southern Ocean were also seen to vary between seasons, with key implications for the ability to assign

an animal to its origin during different seasons. High levels of seasonal variance in isoscapes could potentially improve the potential to assign an animal to a location within an isotopically differentiated area, but reduce the ability to assign an animal to an area in more homogenous months. In any case, knowing the extent and spatial expression of seasonal variation in isoscapes is critical for accurate reconstruction of tropho-spatial ecology (Clive N Trueman et al., 2019). Diet assimilation is also likely to be highly seasonal for higher trophic level organisms, and ideally season-specific isoscapes should be utilised in regions with strong indications for seasonal variability. However, as this is likely not possible in many scenarios, we propose the weighting of mean annual isoscapes by seasonal production to incorporate intra-annual variability.

Using POM to construct stable isotope baselines

POM stable isotope data were used to build the isoscapes presented here, although it should be noted that the suitability of POM as a reference for construction of isoscape models has been widely debated. POM composition and isotopic values can be highly variable in time depending on factors such as nutrient sources (Lara et al., 2010; Stowasser et al., 2012), water column stratification (O'Leary et al., 2001; Zhang et al., 2014), the intensity of primary production (Stowasser et al., 2012), plankton community composition, physiology and growth rates (O'Leary et al., 2001; Trull & Armand, 2001), and microbial and grazing activity (O'Leary et al., 2001). The temporal dynamics of these processes can result in a fast turnover rate and high local variability. Therefore, it has been questioned whether POM provides a suitable baseline over large areas and over medium to long term time scales, which are all requirements in animal tracking studies, for example. There is a practical reason why POM was used to develop isoscapes in this study: these are the only type of data that are numerous enough to offer good spatial coverage and seasonal definition, due to the ease and low

financial costs of sample collection and analysis. By compiling data from a large number of sources and across numerous years and including ‘year’ as a variance term within the INLA model, we hope to have accounted for some of the short-term POM variance.

Secondary producers such as zooplankton may be more appropriate for the generation of isotopic baselines (as a proxy for trophic level two) as they represent a more integrated isotopic signal over space and time, which may be less variable and thus more robust for applications such as animal migration studies. Zooplankton have previously been used to generate carbon and nitrogen isoscapes in regional studies including the Southern Ocean (Graham et al., 2010; McMahon, Hamady, & Thorrold, 2013; Troina et al., 2020; Yang et al., 2020). For this study, however, producing isoscapes based on zooplankton stable isotope values would have resulted in large unsampled areas, and therefore large uncertainties in modelled data. Furthermore, there is no consistency in the species or groups of zooplankton used, which complicates modelling due to variability in, e.g., tissue turnover rates, fractionation and trophic level (Pakhomov, Henschke, Hunt, Stowasser, & Cherel, 2019). Analysis of repeated latitudinal transects across the Southern Ocean have demonstrated that POM stable isotope values tend to be homogeneous across space and time between fronts and associated cross water exchanges created by eddies (B. Espinasse et al., 2019). Overall, it is therefore reasonable to conclude that the high spatial variability predicted in stable isotope values overwhelms the potential variability associated with local changes in POM composition.

CONCLUSIONS

We characterised spatial and temporal variability in the isotopic composition of carbon and nitrogen in POM across the Southern Ocean in greater detail and coverage than it has

previously been achieved. We identified broad spatial and seasonal structure in the recovered isoscape models, providing key evidence for explaining seasonal changes in biogeochemical processes and important implications for using isoscapes for animal assignment applications. We demonstrated that data from numerous sources and years can be combined and modelled to demonstrate these seasonal variabilities. However, the choice of statistical model has substantial impacts on the resultant spatial prediction and associated variability, as well as influencing how isoscape models can be used for future applications. The most accurate isoscape models included first order interactions among the driving variables and were able to predict seasonal isotopic differences in regions with high sampling effort. However, they were associated with higher variability, due to the extrapolation of statistical relationships, relevant in open ocean sectors and in winter months where data are lacking. To improve isoscape accuracy and spatial precision to be able to detect meso-scale features such as eddies, more data are required over further temporal and spatial resolutions. Recognizing the paucity of zooplankton stable isotopic values in the Southern Ocean, future studies should focus on building a unified zooplankton, possible zooplankton based, stable isotope data base to supplement the POM based isoscape modelling efforts.

Acknowledgements

POM data provided by NIWA were collected on RV Tangaroa (TAN) voyages by S. Bury, S. Nodder, A. Gutiérrez-Rodríguez and K. Safi. Funding for sample collection and analysis was provided by the New Zealand Ministry of Business, Innovation and Employment and predecessor science funding agencies, including the Strategic Science Investment Fund to NIWA and the National Coasts & Oceans Centre. Stable isotope analyses from TAN voyages were carried out at the Environmental and Ecological stable Isotope Facility, NIWA Wellington by A. Kilimnik and J. Delgado. Sample collection during the ANT voyages were

done on board the RV ‘Polarstern’ with assistance from M. Brener and L. Gurney. The surveys were financially supported by the German LAKRIS Project (Bundesministerium für Bildung und Forschung, BMBF Forschungsvorhaben 03F0406A/B) and the University of British Columbia (Canada). B. Hunt was funded from the European Union’s Seventh Framework Programme under grant agreement no. 302010 (project ISOZOO) and Natural Sciences and Engineering Research Council of Canada Grant RGPIN-2017-04499. MOBYDICK data sampling was supported by the French oceanographic fleet (“Flotte océanographique française”), ANR program (MOBYDICK Project number: ANR-17-CE01-0013 and the research program of INSU-CNRS LEFE/CYBER (“Les enveloppes fluides et l’environnement”—“Cycles biogéochimiques, environnement et ressources”). POM data provided by Stanford University (R. Dunbar) were collected on voyages of the US NSF operated RVIB Laurence M Gould and Nathaniel B Palmer between 1998 and 2002. All analyses were completed in the Stanford University Stable Isotope Biogeochemistry Laboratory with funding from NSF grants OPP-9615668, OPP-9909837, OPP-0207305, and OPP-1142044 (all to R. Dunbar). This project is supported in part by the Hong Kong Branch of Southern Marine Science and Engineering Guangdong Laboratory (Guangzhou) (SMSEGL20SC02). B. Espinasse is funded from the European Union's Horizon 2020 MSCA program under Grant agreement no. 894296 – Project ISOMOD.

Data availability

All POM SI data used in this study are available as Supporting Information. The isoscapes produced in the present study will be made available on Dryad Digital Repository.

References

Altabet, M. A., & Francois, R. (1994). Sedimentary nitrogen isotopic ratio as a recorder for surface ocean nitrate utilization. *Global Biogeochemical Cycles*, 8(1), 103-116.

- Arteaga, L. A., Boss, E., Behrenfeld, M. J., Westberry, T. K., & Sarmiento, J. L. (2020). Seasonal modulation of phytoplankton biomass in the Southern Ocean. *Nature communications*, 11(1), 5364. doi:10.1038/s41467-020-19157-2
- Barrera, F., Lara, R. J., Krock, B., Garzón-Cardona, J. E., Fabro, E., & Koch, B. P. (2017). Factors influencing the characteristics and distribution of surface organic matter in the Pacific-Atlantic connection. *Journal of Marine Systems*, 175, 36-45.
- Behrenfeld, M. J., & Falkowski, P. G. (1997). Photosynthetic rates derived from satellite-based chlorophyll concentration. *Limnology and Oceanography*, 42(1), 1-20. doi:10.4319/lo.1997.42.1.0001
- Bentaleb, I., Fontugne, M., Descolas-Gros, C., Girardin, C., Mariotti, A., Pierre, C., . . . Poisson, A. (1998). Carbon isotopic fractionation by plankton in the Southern Indian Ocean: relationship between $\delta^{13}\text{C}$ of particulate organic carbon and dissolved carbon dioxide. *Journal of Marine Systems*, 17(1-4), 39-58.
- Bowen, G. J. (2010). Isoscapes: Spatial Pattern in Isotopic Biogeochemistry. *Annual Review of Earth and Planetary Sciences*, 38, 161-187. doi:DOI 10.1146/annurev-earth-040809-152429
- Bowen, G. J., & Revenaugh, J. (2003). Interpolating the isotopic composition of modern meteoric precipitation. *Water Resources Research*, 39(10), 1299.
- Boyd, P. W., Watson, A. J., Law, C. S., Abraham, E. R., Trull, T., Murdoch, R., . . . Zeldis, J. (2000). A mesoscale phytoplankton bloom in the polar Southern Ocean stimulated by iron fertilization. *Nature*, 407(6805), 695-702. doi:10.1038/35037500
- Bracher, A. U., Kroon, B. M. A., & Lucas, M. I. (1999). Primary production, physiological state and composition of phytoplankton in the Atlantic Sector of the Southern Ocean. *Marine Ecology Progress Series*, 190, 1-16. Retrieved from <https://www.int-res.com/abstracts/meps/v190/p1-16/>
- Brault, E. K., Koch, P. L., McMahon, K. W., Broach, K. H., Rosenfield, A. P., Sauthoff, W., . . . Smith, W. O., Jr. (2018). Carbon and nitrogen zooplankton isoscapes in West Antarctica reflect oceanographic transitions. *Marine Ecology Progress Series*, 593, 29-45. Retrieved from <http://www.int-res.com/abstracts/meps/v593/p29-45/>
- Bury, S. J., Pinkerton, M., Sabadel, A., Peters, K., St. John Glew, K., Escobar-Flores, P., . . . Double, M. (In Prep). Stable isotopes elucidate diet and feeding locations of Southern Ocean humpback whales (*Megaptera novaeangliae*) sampled around the Balleny Islands, Antarctica.
- Bury, S. J., Pinkerton, M. H., Williams, M., St John Glew, K., & Trueman, C. N. (in review). Drivers of hydrographic and isotopic variability in surface waters from New Zealand to Ross Sea: validation of south-west Pacific and Southern Ocean isoscapes. *Deep Sea Research Part A. Oceanographic Research Papers*.
- Carreto, J. I., Montoya, N. G., Carignan, M. O., Akselman, R., Acha, E. M., & Derisio, C. (2016). Environmental and biological factors controlling the spring phytoplankton bloom at the Patagonian shelf-break front – Degraded fucoxanthin pigments and the importance of microzooplankton grazing. *Progress in Oceanography*, 146, 1-21. doi:<https://doi.org/10.1016/j.pocean.2016.05.002>
- Ceia, F. R., Ramos, J. A., Phillips, R. A., Cherel, Y., Jones, D. C., Vieira, R. P., & Xavier, J. C. (2015). Analysis of stable isotope ratios in blood of tracked wandering albatrosses fails to distinguish a $\delta^{13}\text{C}$ gradient within their winter foraging areas in the southwest Atlantic Ocean. *Rapid Communications in Mass Spectrometry*, 29(24), 2328-2336.
- Cherel, Y., & Hobson, K. A. (2007). Geographical variation in carbon stable isotope signatures of marine predators: a tool to investigate their foraging areas in the Southern Ocean. *Marine Ecology Progress Series*, 329, 281-287. Retrieved from <https://www.int-res.com/abstracts/meps/v329/p281-287/>
- Darnaude, A. M., & Hunter, E. (2018). Validation of otolith $\delta^{18}\text{O}$ values as effective natural tags for shelf-scale geolocation of migrating fish. *Marine Ecology Progress Series*, 598, 167-185. Retrieved from <https://www.int-res.com/abstracts/meps/v598/p167-185/>
- Dehairs, F., Kopczynska, E., Nielsen, P., Lancelot, C., Bakker, D., Koeve, W., & Goeyens, L. (1997). $\delta^{13}\text{C}$ of Southern Ocean suspended organic matter during spring and early summer: regional and temporal variability. *Deep Sea Research Part II: Topical Studies in Oceanography*, 44(1-2), 129-142.

- Deniro, M. J., & Epstein, S. (1981). Influence of diet on the distribution of nitrogen isotopes in animals. *Geochimica et Cosmochimica Acta*, 45(3), 341-351. doi:[https://doi.org/10.1016/0016-7037\(81\)90244-1](https://doi.org/10.1016/0016-7037(81)90244-1)
- Deppeler, S. L., & Davidson, A. T. (2017). Southern Ocean phytoplankton in a changing climate. *Frontiers in Marine Science*, 4, 40.
- Deuser, W. G. (1970). Isotopic Evidence for Diminishing Supply of Available Carbon during Diatom Bloom in the Black Sea. *Nature*, 225(5237), 1069-1071. doi:10.1038/2251069a0
- DiFiore, P. J., Sigman, D. M., Karsh, K. L., Trull, T. W., Dunbar, R. B., & Robinson, R. S. (2010). Poleward decrease in the isotope effect of nitrate assimilation across the Southern Ocean. *Geophysical Research Letters*, 37(17). doi:10.1029/2010GL044090
- Durack, P. J., & Wijffels, S. E. (2010). Fifty-year trends in global ocean salinities and their relationship to broad-scale warming. *Journal of Climate*, 23(16), 4342-4362.
- Eadie, B. J., & Jeffrey, L. M. (1973). $\delta^{13}\text{C}$ analyses of oceanic particulate organic matter. *Marine Chemistry*, 1(3), 199-209.
- El-Sabaawi, R. W., Trudel, M., Mackas, D. L., Dower, J. F., & Mazumder, A. (2012). Interannual variability in bottom-up processes in the upstream range of the California Current system: An isotopic approach. *Progress in Oceanography*, 106, 16-27. doi:<http://dx.doi.org/10.1016/j.pocean.2012.06.004>
- Eppley, R. W. (1972). Temperature and phytoplankton growth in the sea. *Fishery Bulletin*, 70, 1063-1085.
- Espinasse, B., Hunt, B. P., Batten, S. D., & Pakhomov, E. A. (2020). Defining isoscapes in the Northeast Pacific as an index of ocean productivity. *Global Ecology and Biogeography*, 29(2), 246-261.
- Espinasse, B., Pakhomov, E. A., Hunt, B. P. V., & Bury, S. J. (2019). Latitudinal gradient consistency in carbon and nitrogen stable isotopes of particulate organic matter in the Southern Ocean. *Marine Ecology Progress Series*, 631, 19-30. Retrieved from <https://www.int-res.com/abstracts/meps/v631/p19-30/>
- Francois, R., Altabet, M. A., Goericke, R., McCorkle, D. C., Brunet, C., & Poisson, A. (1993). Changes in the $\delta^{13}\text{C}$ of surface water particulate organic matter across the subtropical convergence in the SW Indian Ocean. *Global Biogeochemical Cycles*, 7(3), 627-644.
- Franks, P. J. S. (2015). Has Sverdrup's critical depth hypothesis been tested? Mixed layers vs. turbulent layers. *ICES Journal of Marine Science*, 72(6), 1897-1907. doi:10.1093/icesjms/fsu175
- Fripiat, F., Sigman, D. M., Fawcett, S. E., Rafter, P. A., Weigand, M. A., & Tison, J. L. (2014). New insights into sea ice nitrogen biogeochemical dynamics from the nitrogen isotopes. *Global Biogeochemical Cycles*, 28(2), 115-130. doi:10.1002/2013GB004729
- Giménez, E. M., Winkler, G., Hoffmeyer, M., & Ferreyra, G. A. (2018). Composition, spatial distribution, and trophic structure of the zooplankton community in San Jorge Gulf, southwestern Atlantic Ocean. *Oceanography*, 31(4), 154-163.
- Goericke, R., & Fry, B. (1994). Variations of marine plankton $\delta^{13}\text{C}$ with latitude, temperature, and dissolved CO_2 in the world ocean. *Global Biogeochemical Cycles*, 8(1), 85-90. doi:10.1029/93GB03272
- Graham, B. S., Koch, P. L., Newsome, S. D., McMahon, K. W., & Auriolos, D. (2010). Using isoscapes to trace the movements and foraging behavior of top predators in oceanic ecosystems. In J. B. West, G. J. Bowen, T. E. Dawson, & K. P. Tu (Eds.), *Isoscapes: Understanding movement, pattern, and process on Earth through isotope mapping* (pp. 299-318). Dordrecht: Springer.
- Gruber, N., Keeling, C. D., Bacastow, R. B., Guenther, P. R., Lueker, T. J., Wahlen, M., . . . Stocker, T. F. (1999). Spatiotemporal patterns of carbon-13 in the global surface oceans and the oceanic suess effect. *Global Biogeochemical Cycles*, 13(2), 307-335. doi:10.1029/1999GB900019
- Guinehut, S., Dhomps, A. L., Larnicol, G., & Le Traon, P. Y. (2012). High resolution 3-D temperature and salinity fields derived from in situ and satellite observations. *Ocean Science*, 8(5), 845-857. doi:10.5194/os-8-845-2012

- Henley, S. F., Cavan, E. L., Fawcett, S. E., Kerr, R., Monteiro, T., Sherrell, R. M., . . . Schloss, I. R. (2020). Changing biogeochemistry of the Southern Ocean and its ecosystem implications. *Frontiers in Marine Science*, 7, 581.
- Henley, S. F., Cavan, E. L., Fawcett, S. E., Kerr, R., Monteiro, T., Sherrell, R. M., . . . Smith, S. (2020). Changing Biogeochemistry of the Southern Ocean and Its Ecosystem Implications. *Frontiers in Marine Science*, 7(581). doi:10.3389/fmars.2020.00581
- Hofmann, M., Wolf-Gladrow, D. A., Takahashi, T., Sutherland, S. C., Six, K. D., & Maier-Reimer, E. (2000). Stable carbon isotope distribution of particulate organic matter in the ocean: a model study. *Marine Chemistry*, 72(2), 131-150.
- Horii, S., Takahashi, K., Shiozaki, T., Hashihama, F., & Furuya, K. (2018). Stable isotopic evidence for the differential contribution of diazotrophs to the epipelagic grazing food chain in the mid-Pacific Ocean. *Global Ecology and Biogeography*, 27(12), 1467-1480.
- Hussey, N. E., MacNeil, M. A., McMeans, B. C., Olin, J. A., Dudley, S. F. J., Cliff, G., . . . Fisk, A. T. (2014). Rescaling the trophic structure of marine food webs. *Ecology Letters*, 17(2), 239-250. doi:10.1111/ele.12226
- Jaeger, A., Lecomte, V. J., Weimerskirch, H., Richard, P., & Cherel, Y. (2010). Seabird satellite tracking validates the use of latitudinal isoscapes to depict predators' foraging areas in the Southern Ocean. *Rapid Communications in Mass Spectrometry*, 24(23), 3456-3460. doi:10.1002/rcm.4792
- Jennings, S., & Warr, K. J. (2003). Environmental correlates of large-scale spatial variation in the $\delta^{15}\text{N}$ of marine animals. *Marine Biology*, 142(6), 1131-1140. doi:10.1007/s00227-003-1020-0
- Kennedy, H., & Robertson, J. (1995). Variations in the isotopic composition of particulate organic carbon in surface waters along an 88 W transect from 67 S to 54 S. *Deep Sea Research Part II: Topical Studies in Oceanography*, 42(4-5), 1109-1122.
- Kennicutt, M. C., Chown, S. L., Cassano, J. J., Liggett, D., Massom, R., Peck, L. S., . . . Wilson, T. J. (2014). Polar research: six priorities for Antarctic science. *Nature News*, 512(7512), 23.
- Klein, E. S., Hill, S. L., Hinke, J. T., Phillips, T., & Watters, G. M. (2018). Impacts of rising sea temperature on krill increase risks for predators in the Scotia Sea. *PloS One*, 13(1), e0191011.
- Kline Jr, T. C. (2009). Characterization of carbon and nitrogen stable isotope gradients in the northern Gulf of Alaska using terminal feed stage copepodite-V *Neocalanus cristatus*. *Deep Sea Research Part II: Topical Studies in Oceanography*, 56(24), 2537-2552. doi:<http://dx.doi.org/10.1016/j.dsr2.2009.03.004>
- Kurle, C. M., & McWhorter, J. K. (2017). Spatial and temporal variability within marine isoscapes: implications for interpreting stable isotope data from marine systems. *Marine Ecology Progress Series*, 568, 31-45.
- Lannuzel, D., Chever, F., van der Merwe, P. C., Janssens, J., Roukaerts, A., Cavagna, A.-J., . . . Meiners, K. M. (2016). Iron biogeochemistry in Antarctic pack ice during SIPEX-2. *Deep Sea Research Part II: Topical Studies in Oceanography*, 131, 111-122. doi:<https://doi.org/10.1016/j.dsr2.2014.12.003>
- Lara, R. J., Alder, V., Franzosi, C. A., & Kattner, G. (2010). Characteristics of suspended particulate organic matter in the southwestern Atlantic: Influence of temperature, nutrient and phytoplankton features on the stable isotope signature. *Journal of Marine Systems*, 79(1), 199-209. doi:<https://doi.org/10.1016/j.jmarsys.2009.09.002>
- Laws, E. A., Bidigare, R. R., & Popp, B. N. (1997). Effect of growth rate and CO_2 concentration on carbon isotopic fractionation by the marine diatom *Phaeodactylum tricornutum*. *Limnology and Oceanography*, 42(7), 1552-1560. Retrieved from <Go to ISI>://WOS:000072822100007
- Lee, S. H., Schell, D. M., McDonald, T. L., & Richardson, W. J. (2005). Regional and seasonal feeding by bowhead whales *Balaena mysticetus* as indicated by stable isotope ratios. *Marine Ecology Progress Series*, 285, 271-287.
- Li, W. K., McLaughlin, F. A., Lovejoy, C., & Carmack, E. C. (2009). Smallest algae thrive as the Arctic Ocean freshens. *Science*, 326(5952), 539-539.
- Loeb, V., Siegel, V., Holm-Hansen, O., Hewitt, R., Fraser, W., Trivelpiece, W., & Trivelpiece, S. (1997). Effects of sea-ice extent and krill or salp dominance on the Antarctic food web. *Nature*, 387(6636), 897-900.

- Lourey, M. J., Trull, T. W., & Sigman, D. M. (2003). Sensitivity of $\delta^{15}\text{N}$ of nitrate, surface suspended and deep sinking particulate nitrogen to seasonal nitrate depletion in the Southern Ocean. *Global Biogeochemical Cycles*, 17(3).
- Lourey, M. J., Trull, T. W., & Tilbrook, B. (2004). Sensitivity of $\delta^{13}\text{C}$ of Southern Ocean suspended and sinking organic matter to temperature, nutrient utilization, and atmospheric CO_2 . *Deep Sea Research Part I: Oceanographic Research Papers*, 51(2), 281-305.
- MacKenzie, K. M., Longmore, C., Preece, C., Lucas, C. H., & Trueman, C. N. (2014). Testing the long-term stability of marine isoscapes in shelf seas using jellyfish tissues. *Biogeochemistry*, 121(2), 441-454. doi:10.1007/s10533-014-0011-1
- Magozzi, S., Yool, A., Zanden, H. B. V., Wunder, M. B., & Trueman, C. N. (2017). Using ocean models to predict spatial and temporal variation in marine carbon isotopes. *Ecosphere*, 8(5), e01763. doi:10.1002/ecs2.1763
- Maritorena, S., d'Andon, O. H. F., Mangin, A., & Siegel, D. A. (2010). Merged satellite ocean color data products using a bio-optical model: Characteristics, benefits and issues. *Remote Sensing of Environment*, 114(8), 1791-1804. doi:<https://doi.org/10.1016/j.rse.2010.04.002>
- Martin, J. H. (1990). Glacial-interglacial CO_2 change: The Iron Hypothesis. *Paleoceanography*, 5(1), 1-13. doi:<https://doi.org/10.1029/PA005i001p00001>
- McMahon, K. W., Hamady, L. L., & Thorrold, S. R. (2013). A review of ecogeochemistry approaches to estimating movements of marine animals. *Limnology and Oceanography*, 58(2), 697-714. doi:10.4319/lo.2013.58.2.0697
- Montecinos, S., Castro, L. R., & Neira, S. (2016). Stable isotope ($\delta^{13}\text{C}$ and $\delta^{15}\text{N}$) and trophic position of Patagonian sprat (*Sprattus fuegensis*) from the Northern Chilean Patagonia. *Fisheries Research*, 179, 139-147.
- Montoya, J. P., Carpenter, E. J., & Capone, D. G. (2002). Nitrogen fixation and nitrogen isotope abundances in zooplankton of the oligotrophic North Atlantic. *Limnology and Oceanography*, 47(6), 1617-1628.
- Morel, A. (1991). Light and marine photosynthesis: a spectral model with geochemical and climatological implications. *Progress in Oceanography*, 26(3), 263-306. doi:[https://doi.org/10.1016/0079-6611\(91\)90004-6](https://doi.org/10.1016/0079-6611(91)90004-6)
- Munro, D. R., Dunbar, R. B., Mucciarone, D. A., Arrigo, K. R., & Long, M. C. (2010). Stable isotope composition of dissolved inorganic carbon and particulate organic carbon in sea ice from the Ross Sea, Antarctica. *Journal of Geophysical Research: Oceans*, 115(C9). doi:10.1029/2009JC005661
- O'Leary, T., Trull, T., Griffiths, F., Tilbrook, B., & Revill, A. (2001). Euphotic zone variations in bulk and compound-specific $\delta^{13}\text{C}$ of suspended organic matter in the Subantarctic Ocean, south of Australia. *Journal of Geophysical Research: Oceans*, 106(C12), 31669-31684.
- Orsi, A. H., & Harris, U. (2019). *Fronts of the Antarctic Circumpolar Current - GIS data*. Retrieved from: https://data.aad.gov.au/metadata/records/antarctic_circumpolar_current_fronts, <https://researchdata.edu.au/fronts-antarctic-circumpolar-current-gis>
- Pakhomov, E. A., Henschke, N., Hunt, B. P., Stowasser, G., & Cherel, Y. (2019). Utility of salps as a baseline proxy for food web studies. *Journal of Plankton Research*, 41(1), 3-11.
- Pethybridge, H., Choy, C. A., Logan, J. M., Allain, V., Lorrain, A., Bodin, N., . . . Olson, R. J. (2018). A global meta-analysis of marine predator nitrogen stable isotopes: Relationships between trophic structure and environmental conditions. *Global Ecology and Biogeography*, 27(9), 1043-1055. doi:10.1111/geb.12763
- Popp, B. N., Trull, T., Kenig, F., Wakeham, S. G., Rust, T. M., Tilbrook, B., . . . Bidigare, R. R. (1999). Controls on the carbon isotopic composition of Southern Ocean phytoplankton. *Global Biogeochemical Cycles*, 13(4), 827-843.
- Post, D. M. (2002). Using Stable Isotopes to Estimate Trophic Position: Models, Methods, and Assumptions. *Ecology*, 83(3), 703-718. doi:10.2307/3071875
- Quillfeldt, P., Masello, J. F., McGill, R. A. R., Adams, M., & Furness, R. W. (2010). Moving polewards in winter: a recent change in the migratory strategy of a pelagic seabird? *Frontiers in Zoology*, 7, 15. doi:ArtN 15
- Doi 10.1186/1742-9994-7-15

- Rau, G., Takahashi, T., Des Marais, D., & Sullivan, C. (1991). Particulate organic matter $\delta^{13}\text{C}$ variations across the Drake Passage. *Journal of Geophysical Research: Oceans*, 96(C8), 15131-15135.
- Rau, G. H., Low, C., Pennington, J. T., Buck, K. R., & Chavez, F. P. (1998). Suspended particulate nitrogen $\delta^{15}\text{N}$ versus nitrate utilization: observations in Monterey Bay, CA. *Deep Sea Research Part II: Topical Studies in Oceanography*, 45(8), 1603-1616. doi:[https://doi.org/10.1016/S0967-0645\(98\)80008-8](https://doi.org/10.1016/S0967-0645(98)80008-8)
- Reiss, C. S., Cossio, A., Santora, J. A., Dietrich, K. S., Murray, A., Mitchell, B. G., . . . Jones, C. D. (2017). Overwinter habitat selection by Antarctic krill under varying sea-ice conditions: implications for top predators and fishery management. *Marine Ecology Progress Series*, 568, 1-16.
- Riaux-Gobin, C., Fontugne, M., Jensen, K., Bentaleb, I., Cauwet, G., Chrétiennot-Dinet, M.-J., & Poisson, A. (2006). Surficial deep-sea sediments across the polar frontal system (Southern Ocean, Indian sector): Particulate carbon content and microphyte signatures. *Marine Geology*, 230(3-4), 147-159.
- Richoux, N. B., & Froneman, P. W. (2009). Plankton trophodynamics at the subtropical convergence, Southern Ocean. *Journal of Plankton Research*, 31(9), 1059-1073.
- Riebesell, U., Burkhardt, S., Dauelsberg, A., & Kroon, B. (2000). Carbon isotope fractionation by a marine diatom: dependence on the growth-rate-limiting resource. *Marine ecology. Progress series*, 193, 295-303.
- Rogers, A., Frinault, B., Barnes, D., Bindoff, N., Downie, R., Ducklow, H., . . . Hofmann, E. (2020). Antarctic futures: an assessment of climate-driven changes in ecosystem structure, function, and service provisioning in the Southern Ocean. *Annual Review of Marine Science*, 12, 87-120.
- Rolff, C. (2000). Seasonal variation in $\delta^{13}\text{C}$ and $\delta^{15}\text{N}$ of size-fractionated plankton at a coastal station in the northern Baltic proper. *Marine Ecology Progress Series*, 203, 47-65. doi:10.3354/meps203047
- Rue, H., Martino, S., & Chopin, N. (2009). Approximate Bayesian inference for latent Gaussian models using integrated nested Laplace approximations (with discussion). *Journal of the Royal Statistical Society, Series B*, 71, 319-392.
- Ryabenko, E. (2013). Stable isotope methods for the study of the nitrogen cycle. In E. Zambianchi (Ed.), *Topics in Oceanography*: InTech.
- Sakamoto, T., Komatsu, K., Shirai, K., Higuchi, T., Ishimura, T., Setou, T., . . . Kawabata, A. (2018). Combining microvolume isotope analysis and numerical simulation to reproduce fish migration history. *Methods in Ecology and Evolution*, 0(0). doi:10.1111/2041-210X.13098
- Schmidt, K., Atkinson, A., Stübing, D., McClelland, J. W., Montoya, J. P., & Voss, M. (2003). Trophic relationships among Southern Ocean copepods and krill: some uses and limitations of a stable isotope approach. *Limnology and Oceanography*, 48(1), 277-289.
- Schofield, O., Ducklow, H. W., Martinson, D. G., Meredith, M. P., Moline, M. A., & Fraser, W. R. (2010). How Do Polar Marine Ecosystems Respond to Rapid Climate Change? *Science*, 328(5985), 1520. doi:10.1126/science.1185779
- Seyboth, E., Botta, S., Mendes, C. R. B., Negrete, J., Dalla Rosa, L., & Secchi, E. R. (2018). Isotopic evidence of the effect of warming on the northern Antarctic Peninsula ecosystem. *Deep Sea Research Part II: Topical Studies in Oceanography*, 149, 218-228. doi:<https://doi.org/10.1016/j.dsr2.2017.12.020>
- Sokolov, S., & Rintoul, S. R. (2009). Circumpolar structure and distribution of the Antarctic Circumpolar Current fronts: 1. Mean circumpolar paths. *Journal of Geophysical Research: Oceans*, 114(C11). doi:10.1029/2008JC005108
- Somes, C. J., Schmittner, A., Galbraith, E. D., Lehmann, M. F., Altabet, M. A., Montoya, J. P., . . . Eby, M. (2010). Simulating the global distribution of nitrogen isotopes in the ocean. *Global Biogeochemical Cycles*, 24, GB4019 doi: 10.1029/2009GB003767
- St John Glew, K., Wanless, S., Harris, M. P., Daunt, F., Erikstad, K. E., Strøm, H., & Trueman, C. N. (2018). Moulting location and diet of auks in the North Sea inferred from coupled light-based and isotope-based geolocation. *Marine Ecology Progress Series*, 599, 239-251. Retrieved from <https://www.int-res.com/abstracts/meps/v599/p239-251/>

- St. John Glew, K., Graham, L. J., McGill, R. A., & Trueman, C. N. (2019). Spatial models of carbon, nitrogen and sulphur stable isotope distributions (isoscapes) across a shelf sea: An INLA approach. *Methods in Ecology and Evolution*, 00, 1-14.
- Stowasser, G., Atkinson, A., McGill, R., Phillips, R., Collins, M. A., & Pond, D. (2012). Food web dynamics in the Scotia Sea in summer: a stable isotope study. *Deep Sea Research Part II: Topical Studies in Oceanography*, 59, 208-221.
- Strutton, P., Lovenduski, N., Mongin, M., & Matear, R. (2012). Quantification of Southern Ocean phytoplankton biomass and primary productivity via satellite observations and biogeochemical models. *CCAMLR Science*, 19, 247-265.
- Swart, N. C., Gille, S. T., Fyfe, J. C., & Gillett, N. P. (2018). Recent Southern Ocean warming and freshening driven by greenhouse gas emissions and ozone depletion. *Nature Geoscience*, 11(11), 836-841.
- Switzer, A. C., Kamykowski, D., & Zentara, S. J. (2003). Mapping nitrate in the global ocean using remotely sensed sea surface temperature. *Journal of Geophysical Research: Oceans*, 108(C8).
- Tagliabue, A., Bowie, A. R., Boyd, P. W., Buck, K. N., Johnson, K. S., & Saito, M. A. (2017). The integral role of iron in ocean biogeochemistry. *Nature*, 543(7643), 51-59. doi:10.1038/nature21058
- Trebilco, R., Melbourne-Thomas, J., & Constable, A. J. (2020). The policy relevance of Southern Ocean food web structure: Implications of food web change for fisheries, conservation and carbon sequestration. *Marine Policy*, 103832.
- Troina, G. C., Dehairs, F., Botta, S., Di Tullio, J. C., Elskens, M., & Secchi, E. R. (2020). Zooplankton-based $\delta^{13}\text{C}$ and $\delta^{15}\text{N}$ isoscapes from the outer continental shelf and slope in the subtropical western South Atlantic. *Deep Sea Research Part I: Oceanographic Research Papers*, 103235.
- Trueman, C. N., Jackson, A. L., Chadwick, K. S., Coombs, E. J., Feyrer, L. J., Magozzi, S., . . . Cooper, N. (2019). Combining simulation modeling and stable isotope analyses to reconstruct the last known movements of one of Nature's giants. *PeerJ*, 7, e7912.
- Trueman, C. N., MacKenzie, K. M., & Palmer, M. R. (2012). Identifying migrations in marine fishes through stable-isotope analysis. *Journal of Fish Biology*, 81(2), 826-847. doi:10.1111/j.1095-8649.2012.03361.x
- Trueman, C. N., & St John Glew, K. (2019). Isotopic tracking of marine animal movement. In *Tracking Animal Migration with Stable Isotopes* (pp. 137-172): Elsevier.
- Trull, T., & Armand, L. (2001). Insights into Southern Ocean carbon export from the $\delta^{13}\text{C}$ of particles and dissolved inorganic carbon during the SOIREE iron release experiment. *Deep Sea Research Part II: Topical Studies in Oceanography*, 48(11), 2655-2680.
- Wada, E., Terazaki, M., Kabaya, Y., & Nemoto, T. (1987). ^{15}N and ^{13}C abundances in the Antarctic Ocean with emphasis on the biogeochemical structure of the food web. *Deep Sea Research Part A. Oceanographic Research Papers*, 34(5-6), 829-841.
- Wunder, M. B. (2010). Using isoscapes to model probability surfaces for determining geographic origins. In J. B. West, G. J. Bowen, T. E. Dawson, & K. P. Tu (Eds.), *Isoscapes: Understanding movement, pattern, and process on Earth through isotope mapping* (pp. 251-270). Dordrecht: Springer.
- Yang, G., Atkinson, A., Hill, S. L., Guglielmo, L., Granata, A., & Li, C. (2020). Changing circumpolar distributions and isoscapes of Antarctic krill: Indo-Pacific habitat refuges counter long-term degradation of the Atlantic sector. *Limnology and Oceanography*.
- Zhang, R., Zheng, M., Chen, M., Ma, Q., Cao, J., & Qiu, Y. (2014). An isotopic perspective on the correlation of surface ocean carbon dynamics and sea ice melting in Prydz Bay (Antarctica) during austral summer. *Deep Sea Research Part I: Oceanographic Research Papers*, 83, 24-33. doi:<https://doi.org/10.1016/j.dsr.2013.08.006>